Evaluating and Extending the Ocean Wind Climate Data Record

Frank J. Wentz[1], Lucrezia Ricciardulli[1], Ernesto Rodriguez[2], Bryan Stiles[2],

Mark Bourassa[3], David Long[4], Ross Hoffman[5], Ad Stoffelen[6], Anton Verhoef[6],

Larry O'Neill[7], Tom Farrar[8], Douglas Vandemark[9], Alexander Fore[2],

Svetla Hristova Veleva[2], Joe Turk[2], Robert Gaston[2], Douglas Tyler[2]

[1]Remote Sensing Systems, Santa Rosa, CA, 95401, USA

[2]Jet Propulsion Laboratory, Pasadena, CA, 91109, USA

[3]Florida State University, Tallahassee, FL 32306, USA

[4]Brigham Young University, Provo, UT, 84062, USA

[5]NOAA-Atlantic Oceanographic and Meteorological Laboratory, Miami, FL 33149, USA

[6]Royal Netherlands Meteorological Institute, De Bilt, Netherlands

[7]Oregon State University, Corvallis, OR 97331, USA

[8]Woods Hole Oceanographic Institution, Woods Hole, MA 02543, USA

[9]University of New Hampshire, Durham, NH 03824, USA

Abstract

Satellite microwave sensors, both active scatterometers and passive radiometers, have been systematically measuring near-surface ocean winds for nearly 40 years, establishing an important legacy in studying and monitoring weather and climate variability. As an aid to such activities, the various wind datasets are being intercalibrated and merged into consistent climate data records (CDRs). The Ocean Wind CDRs (OW-CDRs) are evaluated by comparisons with ocean buoys and intercomparisons among the different satellite sensors and among the different data providers. Extending the OW-CDR into the future requires exploiting all available datasets, such as OSCAT-2 scheduled to launch in July 2016. Three planned methods of calibrating the OSCAT-2 σ_o measurements include (1) direct Ku-band σ_o intercalibration to QuikSCAT and RapidScat, (2) multi-sensor wind speed intercalibration, and (3) calibration to stable rainforest targets. Unfortunately, RapidScat failed in August 2016 and cannot be used to directly calibrate OSCAT-2. A particular future continuity concern is the absence of scheduled new or continuation radiometer missions capable of measuring wind speed. Specialized model assimilations provide 30-year long high temporal/spatial resolution wind vector grids that composite the satellite wind information from OW-CDRs of multiple satellites viewing the Earth at different local times.

Key words—sea surface, radar cross section, remote sensing, satellite applications, wind

1. Introduction

Satellite microwave scatterometers and radiometers have been providing measurements of ocean winds since the launch of the oceanographic satellite SeaSat in 1978. SeaSat flew the SeaSat-A Scatterometer System (SASS) [1] and the Scanning Multichannel Microwave Radiometer (SMMR) [2], but operated for only three months before experiencing a spacecraft

power failure. The radiometric wind speed measurements were continued with a second SMMR flown on the Nimbus-7 spacecraft, also launched in 1978. Scatterometer vector wind measurements did not resume until 1991, when the European Space Agency (ESA) launched its European Remote Sensing Satellite-1 (ERS-1). These early missions have been followed by series of advanced sensors. To present, total of 34 wind-sensing satellite microwave scatterometers and imaging radiometers have been launched.

This paper addresses the challenge of combining wind measurements from this large array of sensors into an accurate representation of the variability of ocean winds over nearly four decades. Ocean winds are a primary driver of the interaction of the planet's atmosphere and oceans, and a true depiction of decadal wind variability is essential to understanding the Earth's climate. The merger and intercalibration of wind retrievals from many sensors (each having its own unique characteristics) spanning several decades is a formidable engineering and scientific endeavor. The desired outcome of this process is a consistent time series of global winds, which is referred to as an ocean wind climate data record (OW-CDR).

OW-CDRs at various stages of development are currently available at a number of institutions. These datasets represent years of careful inter-calibration work required to remove spurious sensor-calibration drifts and inter-sensor biases. Two types of CDRs are available: the ocean vector wind datasets (OVW-CDR) coming from the scatterometers and the wind speed (OWS) only datasets (OWS-CDR) coming from the radiometers. The accuracies of scatterometer and radiometer wind speeds are very similar despite the different measurement technologies. The OWS-CDR can be considered a subset of the OVW-CDR with wind direction missing. Herein, both OVW-CDR and OWS-CDR refer to datasets for which each wind retrieval in the dataset corresponds to an actual satellite measurement.

We also considered higher level ocean wind products for which the OVW-CDRs and the OWS-CDRs are assimilated into a numerical model to construct vector wind fields on a regularly spaced grid in both time and space. The assimilation process usually requires a background field to fill in areas of missing satellite observations. We consider two such products: the cross-calibrated multi-platform (CCMP) dataset and the European Center for Medium-range Weather Forecast (ECMWF) Reanalysis specialized for vector winds (ERA*). The obvious advantage of regularly spaced grids with no gaps needs to be weighed against the loss of linkage to a direct measurement.

Section 2 provides an inventory on the existing and future OVW and OWS datasets extending from 1978 to present. Section 3 discusses the challenge of merging and intercalibrating these wind datasets into a consistent climate data record. Section 4 stresses the importance of maintaining and updating the older datasets. Section 5 discusses various ways of evaluating the OW-CDRs including comparisons with winds from ocean buoys and numerical weather forecast models. This section also emphasizes the importance of having consistent winds from sensors on different satellites. In this pursuit, RapidScat's unique capability of observing ocean vector winds over the complete 24-hour diurnal cycle provides essential information. The section concludes with a plan for comparing OVW datasets from different institutions. Section 6 gives various strategies for extending the OW-CDR into the future, focusing on plans to integrating OSCAT-2 into the OVW-CDR. Section 7 discusses specialized assimilation models designed to provide vector winds on a regular temporal and spatial grid while retaining the satellite wind information. These assimilations can mitigate the long- standing problem of constructing a composite dataset from OW-CDRs of multiple satellites viewing the Earth at different local times.

2. Existing Radiometer OWS and Scatterometer OVW Datasets

Fig. 1, Table 1, and Table 2 show scatterometer and radiometer satellite missions for which wind datasets are available from at least one institution. There are OVW datasets from 13 scatterometers and OWS datasets from 21 imaging radiometers. Of these, four scatterometers and nine radiometers are currently in operation as of November 2016. The figure and tables also include future missions from which wind datasets are anticipated.

WindSat is unique among the satellite radiometers in that it provides both wind speed and direction (i.e. OVWs). This unique capability is due to the inclusion of polarimetric channels that measure ocean brightness temperatures for the 3rd and 4th Stokes parameters, which describe the polarization state of the emitted radiation and are used for wind direction retrievals [3] [4].

Some satellite OW data sets are not included in the figure and tables. Satellite microwave altimeters measure wind speed but with very limited spatial sampling due to their narrow swath (≈5 km) as compared to the imaging radiometers and scatterometers that have swaths between 1000 and 1400 km. Further, an initial comparison of an altimeter OWS-CDR produced by [5] with the SSM/I OWS-CDR [6] showed a large discrepancy, with the altimeter wind trends being 2.5 to 5 times higher than those reported elsewhere [7] [8]. It is unclear if this large discrepancy is due to an inherent sampling and signal-to-noise problems in retrieving altimeter winds or if it is due to correctable problems in the construction of the altimeter OWS-CDR. For these reasons, while altimeters are potentially useful for constructing OWS-CDRs, altimeter CDRs are not included in this paper. In addition, the China National Space Administration (CNSA) Microwave Radiometer Imager (MWRI) hosted on FY and HY spacecraft is not considered here due to quality and availability issues. Another system not included here is CYGNSS, which promises to provide ocean surface winds under all weather conditions from GNSS reflectometry.

3. Climate Data Records for Ocean Winds

As we enter the third decade of satellite wind measurements, the timeline is becoming long enough to characterize the low-frequency decadal oscillations in ocean winds that drive the regional and global exchanges of moisture, momentum, and energy between the planet's oceans and atmosphere. To fully utilize these data sets for climate research, they need to meet the accuracy requirements for a CDR.

The World Meteorological Organization (WMO) Global Climate Observing System (GCOS) accuracy requirement on the OW-CDR is 0.5 m/s for low to moderate winds and 10% for winds exceeding 20 m/s [9]. A stability requirement of 0.1 m/s/decade at global scales is also given. The GCOS temporal and spatial sampling requirements are 10 km and 3 hours. The 10-km resolution requirement is a compromise between a preferred scale of 5 km (or finer) and the reality that satellite sensor technology currently cannot achieve 5 km. A 5-km resolution is greatly preferred for near coastal applications, ocean and atmospheric applications involving curls and divergences, and for near-ice applications.

To meet the temporal requirement of three hours, the International Ocean Vector Wind Science Team (IOVWST) recommended: (1) at least three sun-synchronous scatterometers in orbit; and (2) one additional scatterometer in a non-sun-synchronous orbit (a) to determine the diurnal cycle of wind, (b) to provide better sampling at tropical and mid-latitudes, and (c) to improve sensor intercalibration. These recommendations stem from the demonstrated usefulness of RapidScat observations of the diurnal and semi- diurnal cycle, and the benefits of closer and more plentiful collocations.

With respect to the GCOS stability requirement, the stability of the SSM/I sensors over 20 years was estimated to be 0.05 m/s/decade at the 95% confidence level [6]. More recently, a

relative stability of 0.03 m/s/decade among WindSat, QuikSCAT, and TMI over 10 years was shown in [8]. Thus, it appears that the satellite sensors are meeting the GCOS stability accuracy requirement with a good deal of margin. This is fortunate because the OW-CDR record is now three decades, and the GCOS 0.1 m/s/decade requirement [7] implies a 0.3 m/s drift error over 30 years is acceptable, when it most likely is not. The important role that buoys have to play in verifying long-term stability is discussed in Section 5.

To meet these stringent requirements, the OWS and OVW datasets from the large array of satellite sensors need to be carefully intercalibrated. In addition, the calibration and long- term stability of each sensor need to be assessed and, if required, adjustments be applied. Following this procedure, Remote Sensing Systems (RSS) has produced a 30-year OWS- CDR from 13 satellite radiometers and two scatterometers (QuikSCAT and ASCAT-A) [6] [10] [11] [12]. This CDR begins in 1987 with the launch of the first SSM/I that flew on the DMSP F08 spacecraft. In principle, this wind CDR could be extended back to SeaSat in 1978, but there is a three-year gap (1985-1987) due to the Nimbus-7 SMMR 21 GHz channel failing in March 1985. Due to this gap and to calibration problems with the earlier sensors, the OW-CDR has not yet been extended back to 1978.

Similar efforts are underway at RSS, the Royal Netherlands Meteorological Institute (KNMI), and other institutions to construct OVW-CDRs from the scatterometers measurements [13] [14] [15] [16]. There currently exist partial OVW-CDRs consisting of QuikSCAT and ASCAT-A extending from 1999 to present [17] [18] [16] and there are plans to include ERS-1 and ERS-2 in the CDR [19].

One of the challenges in developing a wind CDR is accounting for diurnal effects. It is well known that ocean winds exhibit significant diurnal variability [20] [21] [22] [23]. When

7

intercalibrating wind sensors on different platforms, this diurnal variation needs to be taken into account. Otherwise, true differences in the wind field due to the diurnal cycle will introduce an aliased diurnal variability signal into the long term timeseries which can be misinterpreted as sensor calibration errors when compared to other sensors. Wind sensors that fly in low inclination orbits, such as TMI, GMI, and RapidScat, can be used to connect the sun-synchronous sensors that observe the oceans at different local times. Using TMI, GMI, and RapidScat, 1-hour collocations can be obtained with each sun-synchronous sensors.

The fact that there are methods for handling diurnal variability for the purpose of inter-sensor calibration does not solve the more fundamental problem of how to incorporate diurnal variability into the OW-CDR. For example, assuming QuikSCAT and ASCAT-A are perfectly intercalibrated from a sensor standpoint, the wind fields from the two sensors are still inconsistent in that they are at four different local times of day (varying with latitude, but at the equator 6 am/pm for QuikSCAT and 9:30 am/pm for ASCAT).

One solution to the diurnal sampling problem is to use numerical assimilation models. These models resample the satellite wind observations to regular (typically 6 hour) time intervals, and hence would be an ideal method to properly account for diurnal information. This is further discussed in Section 7.

Although three to four decades of satellite ocean winds is of enormous value to climate research, extending the record backwards in time to obtain century timescales is of obvious value. The potential of producing a pre-satellite OW-CDR from Volunteer Observing Ships (VOS) observations has been examine by [24]. The visual winds reported by the VOS program are based on the wind-driven sea state, which would be current-relative and related more directly to stress than to wind; implying that visual winds could have dependencies on atmospheric

stability and currents similar to equivalent neutral winds. Visual wind estimates can be used to extend a satellite- like wind climate record back in time, possibly as far back as 1900 in some areas, with the caveats that the VOS sampling is very different from satellite sampling and that the random uncertainty is close to 3 m/s [22].

4. Maintaining and Updating the Older OW Datasets

The scientific value of the OW-CDR is highly dependent on the length of the record, and particular attention needs to be paid to the older data sets, some going back 40 years. In general, these older datasets are given much less priority than OW datasets coming from newer sensors. It should be recognized that the ocean wind retrievals at the beginning of the CDR have equal scientific importance as those at the end of the record. Accordingly, the older datasets need to be actively maintained and periodically improved else the scientific value of these historical datasets will become obscure and loose value relative to newly produced datasets. The individual datasets in the CDR are sometimes reprocessed for a series of reasons, i.e. emergence of sensor calibration issues, improvements in the geophysical model functions (GMFs) or in the wind algorithms, enhanced quality control. Each time one dataset is reprocessed, all the other wind datasets need to be revised and possibly updated too, to make sure their calibration is still in line with all other datasets in the CDR. This process requires a meticulous validation of multi-year wind timeseries and the statistical features of each sensor's wind speed and direction versus quality-controlled ground truth (i.e. buoys, aircraft data, dropsondes, Numerical Weather Prediction models, NWP, or other satellite data).

While making the wind datasets available from a NASA data center is a good first step, more is required. Proactive encouragement and support for version updates and scientific

advocacy are needed. By scientific advocacy, we mean explaining and demonstrating the value of these older data to the Earth Science Community at large. Without version updates and advocacy the older datasets lose consistency with newer datasets, and the value of the combined datasets will be diminished. Instead, we need the sum of the components to have greater value, resulting from consistent datasets useful for long-term studies.

As time goes on, we will better understand how to extract more information from the past and present scatterometer/radiometermeasurements.Improved geophysical model functions (GMF) with extended parametrizations will be developed, and more advanced inverse methods (i.e., retrieval algorithms) will be derived. The current lack of proper error characterization of the wind retrievals needs to be remedied. By incorporating more ancillary data (satellite-inferred precipitation, sea-surface temperature, and wave-height) into the retrieval process, the vector wind accuracy will improve. The implementation of these refinements and extensions will require widely publicized version updates, reprocessing, and scientific advocacy on a regular basis of every 3 to 5 years.

The fidelity of satellite intercalibration will also improve with time. We are just beginning to understand the characterization of the wind diurnal cycle using RapidScat and the TMI and GMI radiometers, all flying in rapidly precessing orbits that sample the full 24-hour cycle. The precise removal of small biases between sensors and the detection of slight sensor drifts are improving the extent to which we can now see subtle changes in our climate that are not easily discernable from in situ data. The realization of all these potentials requires establishing a programmatic support mechanism that is focused on maintaining and improving the 30-year archive of satellite winds.

5. Evaluating the OW-CDRS

This section describes various means of evaluating the OW- CDRs. Each method has its advantages and limitations, as summarized here:

1. Comparisons of OW retrievals with buoy winds

   Plus: Provides absolute calibration for wind speed up to 15-20 m/s.

   Minus: Buoy data are spatially very sparse and irregularly distributed; surface currents are not available.

2. Comparisons of OW retrievals with winds from numerical model (such as ECMWF and NCEP)

   Plus: Global comparisons.

   Minus: Systematic errors exist in the numerical analyses and can be large. Analyses often lack or misrepresent the details of mesoscale phenomena.

3. Comparisons of OW retrievals from sensors on two different platforms

   Plus: Direct comparisons of the same wind field; other validation datasets not required.

   Minus: Comparisons are limited by the required tight spatial/temporal collocation.

4. Comparisons of OVW retrievals produced by different data providers

   Plus: Reveals algorithmic uncertainties and deficiencies; validation data not required; no collocation issue.

   Minus: Does not reveal common system errors.

A. Buoy Wind Measurements Provide Absolute Calibration

Moored ocean buoys provide the absolute calibration reference for satellite wind retrievals. While the development of GMF and wind retrieval algorithms rely on many inputs (numerical models, wind retrievals for other satellites, statistical constraints, etc.), the finalized satellite wind retrievals always need to be verified by comparisons with buoys. The buoy comparisons by themselves are not sufficient for complete validation, but they do provide a necessary constraint: when averaged over colocations with a large number of buoys (hundreds)

and for years, the satellite winds need to agree with the buoys for winds below 15-20 m/s. If this condition is not met, then adjustments need to be made to the GMF/retrieval algorithm.

The moored buoy arrays most commonly used for validating satellite winds are the TAO/TRITON array in the tropical Pacific, the PIRATA array in the tropical and subtropical Atlantic Ocean, the RAMA array in the Indian Ocean, and the National Buoy Data Center (NDBC) coastal buoys surrounding the United States (including Hawaii and Alaska). Other buoys are occasionally used, including the coastal buoys maintained by the Canadian Department of Fisheries and Oceans (although the quality control of these wind measurements is less stringent than that applied to the other buoy datasets).

When comparing satellite winds to buoy winds, one must account for (1) the different spatial and temporal sampling of buoy and satellites winds, and (2) The fact that radiometers and scatterometers are actually measuring surface roughness, not the wind. Thus, concerning the latter, one should relate the buoy wind measurements to a surface stress value because it is generally assumed surface stress is the parameter most closely correlated with the wind-induced surface roughness seen by the sensor. The surface stress depends on the velocity difference between the air and ocean and is commonly expressed in terms of the 10-meter equivalent neutral wind (U10EN). This conversion from buoy wind to surface stress must account for the buoy height, atmospheric stability, air mass density, and surface currents [25] [26] [27]. At high winds, buoy measurements become less reliable (e.g., [28]) and are typically excluded from the validation. For the operational buoy network, a high-wind limit of 15 m/s is often used. This limit is based on various buoy analyses [29] [30] [31]. However, with special adjustments for buoy roll and pitch and other factors, the high-wind limit could possibly be extended to 20 or 25 m/s [32].

Buoys are also useful for evaluating satellite winds in rainy areas. Both scatterometers and radiometers are affected by raindrops absorbing and scattering microwaves, as well as impacting the ocean surface roughness. Detailed analyses of collocated scatterometer and buoy vector winds have shown that ASCAT provides much more accurate wind speed and direction estimates in rain than QuikSCAT compared to buoy winds [33] [34] [35] [36]. The reason is that ASCAT operates at C-band, which is less affected by radiative absorption and scattering than Ku-band sensors.

Due to the ephemeral character of tropical convection, there can be large discrepancy between satellite and buoy estimates of temporal wind variability on time scales less than five days. Additionally, individual satellites only observe a given area of the ocean twice a day and therefore are not able to sample the diurnal variability. On timescales greater than five days, the scatterometer datasets provide good estimates of the lower frequency wind variability compared to the buoys, although the possibility exists that there could be small but important biases in rainy regions associated with systematic covariability of rain and wind in precipitating systems.

The need for the absolute wind calibration via ocean buoys will continue into the future. Satellite wind sensors are not perfectly stable, and small drifts in the 30-year OW-CDR observational record are an ongoing concern. In addition, when intercalibrating the numerous satellite sensors, there will be small adjustments applied to wind speeds to bring consistency to the relative intersatellite differences at global scale. These offset errors will propagate like a random walk process, thereby introducing small spurious trends. These effects are expected to be small, as has been demonstrated by various analyzes of satellite data (see Section III). However, keeping the spurious drift below 0.1 m/s over a 30-year span is challenging, and buoys are indispensable for validation.

This continuing need for buoy validation should be clearly communicated to the TPOS 2020 Project, which is currently assessing the future of the ocean buoy network in the tropical Pacific. The number and locations of buoys required for satellite validation need to be specified [37]. An additional challenge in creating a CDR is proper accounting of the uncertainties in each datasets. Ideally, having an error model for each dataset, one could obtain a distribution for the CDR, where the mean serves as the best estimate of the wind field, and the spread relates to its uncertainty. This has yet to be done.

B. Numerical Model Winds Provide a Global Evaluation

Ocean vector winds calculated from today's numerical weather forecast models such as ECMWF, the National Center for Environmental Prediction (NCEP), and the Japanese Meteorological Agency (JMA) provide an accurate representation of the near-surface synoptic-scale ocean wind field. These wind fields are on regularly spaced temporal and spatial grids with no gaps. This grid structure greatly facilitates comparisons with orbiting satellite observations. The numerical models are useful for evaluating wind direction and a reference for wind speed evaluation, but with some caveats. Small systematic regional biases (≈0.5 m/s) between numerical model and satellite winds are typical and should be investigated. The boundary layer physics governing the relationship between the near-surface winds reported by the model and the ocean surface stress measured by the satellites is regionally dependent and is difficult to model at the 0.1 m/s level. In addition, because the quality, quantity, and type of assimilated datasets can change over time, long-term trends coming from numerical model reanalyses may be spurious. For long-term trends, one looks for decadal consistency among the various satellite sensors. Another caveat is that the models may not provide an accurate representation of winds in rainy areas and storms, where small-scale wind features like downdrafts are common.

Numerical model winds are useful for triple collocation analyses with buoy and satellite winds. Since validation datasets also have associated uncertainties, the best way to achieve an estimate of the confidence level for each wind product, satellite, buoy and model wind, is by using a triple- collocation technique [38] [39]. This method compares, in pairs, three mutually-independent wind datasets collocated within a narrow time window. The root-mean-square error for each dataset is found by solving a simple set of three equations. The triple wind speed collocation method can also be applied for different wind speed regimes, to provide a confidence level as a function of wind speed.

C. Consistency in Winds from Sensors on Two Different Platforms

In constructing an OW-CDR, an essential requirement is that the OW from sensors on different satellites agree with each other when the two sensors are observing the same ocean area at the same time. Since exact space/time collocation is rarely achieved, a reasonable space/time collocation window is used. If this window is too large, then systematic diurnal variability and more random mesoscale variability will significantly contribute to real differences in the true vector wind fields. Spatial collocation windows of 25-50 km and temporal windows within 1 hour are typically chosen, as it takes about an hour for an average wind of 7 m/s travel the distance across a satellite footprint. Shorter collocation windows would be ideal, but they collocated data would be very limited in number. For sun-synchronous sensors, achieving a 1-hour collocation with another sensor is problematic, as shown in Figure 2. On the other hand, for convective storm systems, even a 1-hour collocation window is too long [40].

A large time window up to 3 to 6 hours is unavoidable for some applications, and in these cases it must be recognized that the observed OW differences will contain a component that is

not related to sensor/algorithm calibration issues. One possible way to mitigate the problems associated with large time windows is to do a long-term average (i.e., monthly) to reduce the error associated with mesoscale variability. The remaining error due to systematic diurnal variability can possibly be accounted for using a diurnal model of OVW.

The preferred 1-hour collocation window is best achieved utilizing the satellite wind sensors that have inclined orbits like TMI, GMI, and RapidScat. The TMI/GMI combination now extends 19 years starting in 1998, and the RapidScat mission started in 2014 and ended with a permanent power loss in August 2016. These inclined orbits rapidly precess through the diurnal cycle and provide 1-hour or even closer collocations every orbit with all operating sun-synchronous sensors. This approach to intercalibration is further discussed in Section 6.

Intercomparison of winds speeds from two sensors over many years provides an assessment of long-term stability. Fig. 3 shows an example of this. In this figure, ASCAT-A wind speeds are compared to those from eight different satellite sensors. A large 4-hour collocation window is used, but this should not matter for assessing long-term stability as long as the globally averaged wind speed diurnal cycle does not vary in time. Relative to the other satellites, ASCAT appears to be very stable until late 2014, at which time there is a small negative shift ($\approx$ -0.1 m/s) relative to all the other sensors, indicating that the shift can be attributed to an issue with ASCAT-A The ASCAT-A radar cross section has recently been adjusted for this calibration change [41] and the newest wind products take the adjustment into account [42]EUMETSAT and KNMI have confirmed that there were some small issues with the ASCAT-A antenna calibration in the months of September-October 2014, and they determined exact recalibration factors for each antenna using ASCAT-B as a reference in the same sun-synchronous satellite orbit, thus avoiding diurnal cycle effects [41]. Figure 3 also shows a small

drift for SSMI F17 starting in 2017, whose origin is under investigation. Additionally, the figure illustrates how the NCEP wind timeseries contains some spurious biases and drifts due to changes in the assimilated data over time.

Another example of comparing wind speeds from multiple sensors over an extended time period is given by [11]. This analysis uses 1-hour collocations of TMI retrieved wind speeds with 11 other satellite wind sensors. The longest intercomparison was TMI and WindSat, and this pair of sensors show a 0.02 m/s relative drift over the 12 years during which both sensors were in operation.

D. Intercomparison of OVW-CDRs from Different Institutions

By directly comparing OVW retrievals coming from different data providers, the systematic uncertainties due to the various retrieval methodologies and assumptions can be better understood. For this type of analysis, collocation is not a problem, and there is no need for ancillary validation datasets. The spatial and temporal sampling for the two datasets being compared will be the same. Intercomparison of CDRs from different institutions is a standard technique in climate research that has been used extensively in the IPCC Assessment Reports. Notably, the assessment of decadal changes in the Earth's tropospheric and stratospheric temperatures has relied on comparing results from three or four independent institutions [43] [44] [45]. One objective of an OVW intercomparison project is to quantify the differences in the various OWS and OVW datasets so that the uncertainties in the overall retrieval process are better understood. It is anticipated that this will lead to future improvements in OW processing. Prior agreement on a common set of data production criteria is required so that the results from the various institutions can be meaningfully examined.

The production of OVW-CDRs is a complex process consisting of the following components:

1. Calculation of the sea-surface normalized radar cross section σ_o

2. GMF that relates σo to vector wind, incidence angle, and frequency to first order and other parameters to second order

3. Vector wind retrieval algorithm and ambiguity removal algorithm

4. Quality Control (QC), including rain detection and exclusion

5. Spatial and temporal averaging and gridding

For the purpose of intercomparison, the OVW production can be divided into two parts: basic OVW retrieval (components 1-3) and post-processing (components 4-5). There is a close interplay among components 1-3. For example, biases in σo transfer to biases in the GMF such that σ_o – GMF is on the average equal to zero. A thorough description of the methodology adopted for producing each dataset is required so that the OVW differences can be fully understood.

We note that QC is an essential part of the OVW retrieval process and could be included in either the first or second part. The choice of QC procedures can significantly affect intercomparison results. For example, inconsistencies in the rain flags adopted for different wind datasets can result in major inconsistencies in the wind products, even before they are combined into a CDR. Therefore, to simplify the intercomparison among datasets, it is helpful to isolate the effects of steps 1-3 from the QC and averaging procedures. Then a common (consensus) set of procedures for performing steps 4 and 5 can be used to more clearly identify differences in steps 1-3. The impact of QC on OVW can be better understood by performing comparisons for the

same "QC regime". For example, results can be found for four different categories: when both datasets pass the QC, when both fail to pass the QC, and when one or the other passes QC. This stratification allows for a better understanding of the QC in each dataset and eventually should lead to QC improvements, such as more optimal rejection thresholds.

When comparing results for different institutions, a common yet manageable set of evaluation metrics should be adopted. Examples of standard metrics include various statistical representation of the differences Δx in wind speed, wind direction, and the U and V wind components. For example, the mean and standard deviation of Δx can be stratified according to wind speed, SST, latitude, and swath position, and global maps of Δx can be made. Probability density functions of Δx are also a useful analysis tool.

Comparisons can be made on various spatial/temporal scales, ranging from instantaneous vector wind cells, to monthly or yearly 1☐ latitude/longitude maps. A comparison in terms of curl and divergence may be particularly illuminating due to the sensitivity of derivatives to small scales and due to the importance of these wind derivatives for forcing the ocean circulation.

E. Diurnal Cycle, Rain, and High Winds

There are a number of complicating factors that come into play when evaluating OW-CDRs and comparing datasets from different sensors and different institutions. These include (1) the systematic variation of ocean winds over the 24-hour diurnal cycle, (2) the influence of rain of the observations, and (3) high winds (>20 m/s).

The impact of the diurnal cycle is exemplified by comparisons of QuikSCAT and ASCAT. QuikSCAT ascending node (6 am) precedes by few hours ASCAT-A descending node (9:30 am). The variability in ocean winds over the 3.5 hour difference can be large and tends to

confound direct comparisons between QuikSCAT and ASCAT-A, particularly when doing precise analyses at the 0.1 m/s level. Mesoscale variability in the wind field will produce significant random spread in the QuikSCAT-ASCAT differences and the diurnal cycle will produce systematic errors that remain after averaging. Sensors flying in inclined orbits, such as TMI, GMI, and RapidScat, sample the entire diurnal cycle within a month or two and can be used to both determine the natural diurnal variability of winds and remove intersensor biases. Alternatively, NWP model cross-references may be used, which partially capture the diurnal cycle.

The absorption and scattering of microwave by raindrops can have a significant effect on both radiometer and scatterometer measurements. The influence of rain increases with frequency. At L- and C-band the effect is small, but at higher frequencies rain becomes problematic for wind retrievals. In addition, the various retrieval algorithms currently in operation treat rain effects differently. For example, some Ku-band scatterometer retrieval algorithms are designed to partially remove the influence of rain [46] [47] [48] while others rely on an aggressive rain filter to exclude rainy observations [49]. Also, the quality of the numerical model winds (such as ECMWF and NCEP) and the spatial representativeness of buoy winds in rainy areas is questionable, making validation more difficult.

There are several of ways that rain in a scatterometer footprint can be identified. First, rain imparts a discernible signature on the σ_o measurements that provides some information on rain contamination. Second, satellite microwave radiometers provide excellent estimates of rain, but to be useful these observations must be very close in time and space (30-60 minutes, 25 km) to the scatterometer observations. ASCAT on the MetOp missions could benefit from rain-estimates from the Microwave Humidity Sounder. [50] [51] successfully used ASCAT estimates

of high wind variability (MLE and Singularity exponents) to identify areas of rain. These results suggest that it is the wind variability rather than the rain that affects the intercomparison at C-band. Two other useful microwave radiometers for rain-flagging are TMI and GMI, both operating in inclined, non-sun- synchronous orbits. TMI and GMI are therefore able to provide time collocations with the scatterometers at very short time scales, but for limited geographical regions. The CMORPH rain product [52] also provides a useful ancillary dataset for identifying and excluding rain.

In the past, one area of major disagreement between wind speeds produced by different institutions is at winds above 20 m/s. At the High-Winds Workshop held in Miami in December 2015, significant progress was made towards establishing a consensus on the calibration criteria for high winds. Dropsondes in storms can be used as the fundamental calibration reference, and the aircraft Step Frequency Microwave Radiometer (SFMR) can be calibrated to these dropsondes. The SFMR high wind measurements then can be used to develop high-wind GMF for the satellite radiometers and scatterometers.

6. Extending the OW-DCRS into the Future

Fig. 1 shows the currently operating scatterometers and radiometers as well as those planned for future missions. For the scatterometers, ASCAT-A&B, QuikSCAT in its current non-spinning mode, and HY-2A SCAT are being used to extend OVW-CDR forward. Herein, we also discuss plans for using RapidScat to calibrate OSCAT-2 and extended the OW-CDR into the future. However, after submission of the paper, RapidScat suffered a power loss in August 2016.

In addition, there are several new scatterometer missions planned that will carry the OVW-CDR into the future, including:

- ISROs OSCAT-2 on ScatSat (2016) and OSCAT-3 on OceanSat-3 (2018)

- CNSA HSCAT-B on HY-2B (2017) plus follow-on sensors

- ASCAT-C sensor on MetOp-C (2018)

- China Meteorological Administration (CMA) WindRAD (2018)

- Russian SCAT on Meteor-M N3 (2020)

- EUMETSAT SCA on MetOp-SG-B (2022)

Whereas EUMETSAT, ISRO (Indian Space Research Organisation), CNSA, and CMA have made definite commitments to continue wind scatterometers into the future, the same cannot be said for the microwave radiometer wind sensors. The only scheduled sensor is the microwave imager (MWI) for the second-generation MetOp, which is not scheduled to launch until 2022. MWI primary wind sensing channel is 31 GHz, which is less sensitive to wind than the 37 GHz used by previous wind sensors. Currently, there are no commitments from the U.S. for follow-ons to WindSat or GMI, and the Japanese Aerospace Exploration Agency (JAXA) has no commitments for an AMSR-3. While CNSA flies a Microwave Radiometer Imager (MWRI) on the FY and HY spacecraft, the capability of this sensor for accurate and reliable wind retrievals is unclear and wind datasets are not available.

As a result, the continuity of the radiometer OWS-CDR is in jeopardy. Furthermore, in the spring of 2016 the F19 SSM/I failed and the F17 SSM/I 37 GHz v-pol channel became seriously degraded. The OWS-CDR is being extended into the future using the remaining sensors

WindSat, AMSR2, GMI, and possibly the F18 SSM/IS. However, WindSat is well beyond it designed mission life, and AMSR-2 is approaching its designed life. The future of radiometer wind measurements after these sensors cease to function is uncertain. In construction of both the OWS- and OVW-CDRs, an essential requirement is that the wind speeds from sensors on different satellites agree with each other when the two sensors are observing the same ocean area at the same time. For the radiometers, obtaining this multi-sensor consistency in wind speed is achieved by adjusting the brightness temperature (TB) calibration for the various sensors [10] [11] [12]. For the scatterometers, the calibration for the normalized radar cross section (σo) is adjusted (e.g., [41] [19].

In this section, we discuss how the next scatterometer to be launched, OSCAT-2 on ScatSat, will be incorporated into the OVW-CDR. Table 3 summarized the various calibration options. There are plans in place to use all of these calibration methods. By exploiting all options, multiple consistency checks will lead to a well-validated OVW-CDR. In the following subsections, we detail three of these planned OSCAT-2 σ_o calibration. These are: (1) directly comparing OSCAT-2 σ_o measurements with QuikSCAT; (2) adjusting OSCAT-2 σ_o to bring its wind speed retrieval into agreement with other sensors; and (3) comparing OSCAT-2 σ_o rainforest measurements from previous observations.

Results from the three methods can be compared to gain insight into the calibration problem. If all the methods agree within 0.1 dB at global scales, then there is high confidence in the cross-calibration of the sensors. However, one does not expect perfect agreement between methods 1 and 2 because of non-linearities in the wind retrieval algorithm between σ_o and wind speed and other factors as well. In addition, past results have shown small inconsistencies between σ_o calibration using ocean observations as compared to σ_o calibration using rainforest

23

observations. For the first method, one must verify that the σ_o offset does indeed bring consistency to the wind speeds. Often a small residual adjustment, as discussed below, is needed to precisely intercalibrate the wind speed. However, it must be realized that for the determination of an OVW- CDR, consistency in both wind speed and σ_o is important.

A. Direct Intercalibration of Ku-band σo Measurements

Fig. 4 shows a plan for producing a consistent set of Ku- band σ_o measurements starting with QuikSCAT in 1999 and continuing through to OSCAT-2. This intercalibrated 18-year time series of Ku-band σ_o measurements can then be used to produce an OVW-CDR. This method of directly intercalibrating the σ_o measurements (as opposed to intercalibrating wind speeds) has the advantage of providing global calibration information rather than being restricted just to the oceans. Vegetation and soil studies as well as ice research will certainly benefit from two decades of consistent Ku-band observations.

The original plan for the Ku-band σ_o intercalibration was to calibrate RapidScat to the non-spinning QuikSCAT, and then end the QuikSCAT mission and continue with just RapidScat. The inclined orbit of RapidScat (prograde 51.6□ inclination) will give 1-hour collocations with OSCAT-2 every orbit. However, on August 14, 2015, RapidScat suffered a gain anomaly and went into a low signal-to-noise state. The impact of the gain anomaly is still unclear, but it certainly complicates the calibration procedure and brings into question the usefulness of RapidScat for the future calibration of OSCAT-2. In view of RapidScat's uncertain future, NASA decided to extend the QuikSCAT mission through 2017. This proved to be a wise decision in view of the fact that RapidScat shortly thereafter failed.

One key consideration for this calibration method is the long-term stability of QuikSCAT. A technical assessment of the performance and stability of QuikSCAT both before and after the spin mechanism failure is given in the Appendix to [53] and is summarized here. Before the spin mechanism failure, QuikSCAT showed exceptional stability: monitoring the rainforest shows a maximum instrument stability trend of –0.006 dB/year in σo. The stability during normal operation was also demonstrated by comparing QuikSCAT wind speeds with TMI wind speeds. From 1999 to 2009, the relative drift of QuikSCAT minus TMI was only -0.025 m/s [11].

After the instrument stopped spinning, no changes have been noticed in the instrument stability based upon onboard monitoring of observable parameters. The ability to provide calibration using the rainforest is somewhat degraded in the non-spinning state due to the narrow swath and fixed azimuth angles. Based upon the data observed over the Amazon, there is an intrinsic variability of 0.14 dB for 3-day averaging including both spatial-temporal variations in the natural target and instrument noise. The fit of the observed trends in σ_o constrain the maximum instrument term to be less than -0.02 dB/year. QuikSCAT remains the best calibration standard for direct calibration of backscatter cross-section at Ku-band. Based on these numbers, we estimate that OSCAT-2 calibration to better than 0.1 dB level could be done in less than a month. Achieving 0.05 dB would require about three months. Given that the nominal OSCAT-2 data availability starts in August 2016 static calibration using QuikSCAT could be achieved before QuikSCAT enters its eclipse phase in 2016, when science operations pause due to insufficient power. Monitoring OSCAT-2 stability, should that instrument launch late or be unstable in its initial phase, would require QuikSCAT observations after the 2016-2017 eclipse season.

The other important consideration for extending the Ku- band σ_o measurements is the degree to which the RapidScat gain anomaly affects its operation. This issue is also discussed in Appendix to [53] and is summarized here. The ability of RapidScat to serve as a calibration platform was impacted by a hardware degradation that caused the instrument signal-to- noise to drop by about 10 dB. This drop has impacted winds retrievals below 5 m/s and requires new calibration values, which are still being finalized. Nevertheless, for winds higher than 5 m/s and for bright rain forest targets, it is expected that the performance would not be impacted. In spite of the premature end of the RapidScat mission, we expect that the major contribution of RapidScat to OW-CDR will be the diurnal information it provided. This information can be used to tie together observations occurring at different local times of day.

Wind fields from NWP data assimilation systems are insufficient for this purpose because they do not fully resolve scales of motion at resolutions observed by the satellite sensors [54]. In addition, since RapidScat briefly samples at exactly the same local time as all other satellites in the constellation every revolution, it is an invaluable tool for determining regional differences in climate records between different instruments.

RapidScat is the only vector wind sensor that views the ocean throughout the complete 24-hour cycle. This unique capability has great potential for (1) cross-calibrating sun-synchronous sensors and (2) characterizing the diurnal variability of winds over the world's oceans. While there are other methods for cross-calibrating sun-synchronous sensors, there is no substitute for the diurnal vector wind information coming from RapidScat. In view of this, every effort is being made to compensate for the gain anomaly.

B. Intercalibration of Wind Speed via Multiple Sensor Paths

One of the most demanding aspects of producing an OW-CDR is to achieve proper wind speed intercalibration over the large array of sensors that extend nearly 30 years. When OSCAT-2 is launched in mid-2016, there will be about 14 other satellite wind sensors in orbit. For the most part, these 14 sensors will have been intercalibrated and can provide a very reliable wind speed reference for OSCAT-2.

Fig. 5 shows the most reliable calibration paths that can connect the Ku-band OSCAT-2 on ScatSat with the Ku-Band QuikSCAT. There are three paths shown in the figure:

1. QuikSCAT → TMI → ASCAT-A → GMI → OSCAT-2

2. QuikSCAT → TMI → WindSat → GMI → OSCAT-2

3. QuikSCAT → TMI → GMI → OSCAT-2

TMI and GMI are in low inclination orbits, and by using them as connecting sensors, 1-hour collocation windows can be obtained over the entire path. This avoids comparison of observations at different local times, and systematic errors related to the diurnal cycle are greatly mitigated. The local times for QuikSCAT and WindSat are 12 hours apart, and hence a 1-hour collocation window can be used over a good portion of the orbit (ascending orbit segment matching with a descending orbit segment). Thus, a fourth, more direct path can be used:

4. QuikSCAT → WindSat → GMI → OSCAT-2

To assess the error in the wind speed intercalibration method using multiple sensors, Fig. 6 shows global maps of the wind speed difference for ASCAT-A minus GMI and RapidScat minus WindSat. There are some interesting regional features reaching a magnitude of 0.5 m/s in

some places. The cause of these differences is not fully understood, but their standard deviation (not shown) is small (0.1 to 0.2 m/s), and the zonally averaged differences are typically 0.2 m/s and do not exceed 0.3 m/s. For these results, observations in the presence of rain have been excluded using the rain flag provided by the collocated radiometer: WindSat, TMI, or GMI.

The first-order calibration of OSCAT-2 requires applying a calibration offset to the σ_o measurements. Typically, one offset is applied to v-pol and another to h-pol. For the wind-speed calibration method discussed here, the offsets will be determined that remove the wind bias between OSCAT-2 and other available wind sensors, (likely WindSat, GMI, AMSR2, ASCAT-A, and ASCAT-B). This calibration is done by globally averaging the wind speed differences. The global averages of the small regional differences shown in Figure 6 are close to zero.

A similar global wind calibration was done for RapidScat. In this case, the v-pol and h-pol σ_o calibration offsets were found by direct comparisons with the QuikSCAT measurements. Then, when the RapidScat winds coming from the RSS OVW algorithm were compared to WindSat, GMI, AMSR2, and ASCAT-A, a small negative offset of -0.21 m/s was found. Small wind offsets like this are to be expected considering the non-linearities in the σ_o-to-vector wind retrieval algorithm, the particular choice of the GMF, details of the spatial sampling, and uncertainty in the QuikSCAT σ_o measurements used for calibration. The final step in the wind calibration was to remove the -0.21 m/s bias.

Table 4 shows the results of the RapidScat multi-sensor wind calibration. The RapidScat versus WindSat, GMI, AMSR2, and ASCAT-A comparisons show remarkable similarity, with the four different wind offsets only varying from -0.03 to +0.05 m/s. This close agreement is indicative of the success of the current intercalibration procedures for the OW-CDRs.

The calibration paths shown in Fig. 5 highlight the importance of GMI in calibrating OSCAT-2. GMI flies in an inclined orbit (prograde 65° inclination) similar to RapidScat, and 1-hour collocations with OSCAT-2 will be obtained every orbit. GMI has a dual on-board calibration system utilizing both external hot and cold loads and internal noise diodes. This advanced calibration system makes GMI arguably the most accurate satellite microwave radiometer to date [12]. The GMI observations extend from 65°S to 65°N, giving nearly complete coverage of the world's oceans. The GMI wind speed retrievals have been intercalibrated with other sensors and are now consistent with the existing OWS-CDR.

Previous analyses suggest that the σ_o calibration offsets found from the wind-speed calibration method are not necessarily applicable to land and ice observations. The reason for this is not clear, but as a result the wind speed calibration method may not provide sufficiently accurate σ_o calibration over land and ice.

C. Rain Forest Calibration of OSCAT-2

Owing to their constant incidence angles and high degree of accuracy, pencil-beam scatterometer observations such as those from QuikSCAT, Oceansat-2 OSCAT-1, and RapidScat have also found use in various land applications. Most notably, the data have been used in sustaining the long record of sea-ice coverage [55] [56], studying drought conditions [57], and identifying antecedent precipitation [58]. Each of these sensors employs dual beams at similar, but slightly different Earth incidence angles and resolutions.

The brief OSCAT-1 and spinning QuikSCAT overlap period in November 2009 was used by [59] for cross- calibration, but a longer-term Ku-band radar reference is desirable to span the lifetimes of multiple sensors. Beginning in late 1997 with the launch of TRMM, continuous

Ku-band surface backscatter observations have been collected by the NASA/JAXA Precipitation Radar (PR) (science operations ended in late 2014), and the GPM Dual-Frequency Precipitation Radar (DPR) (March 2014-current), giving an approximate 9-month overlap period. Since the time record covers all scatterometer missions mentioned above, these observations could potentially serve as a source for long-term cross-referencing between individual scatterometer sensors.

The variability in the multispectral σ_o (including TRMM/PR) over several land surface types was studied by [60]. For scatterometer cross-calibration, a complication arises since both the PR and DPR radars scan an approximate 240- km swath at 49 incidence angles between $\pm 17°$ about nadir, unlike the viewing angle range of the scatterometers mentioned above which fall between the range of 45° and 55°. Over most land surfaces, the high variability of the near-nadir backscatter [61] limits the utility of these data for cross- referencing. The exception is for dense-enough vegetation, such as that found in the rainforests in the Amazon, the Congo and other similar locations, where the backscatter is fairly constant for angles greater than 10°-15° from nadir. This behavior is illustrated in Fig. 7, which contrasts the off-nadir Ku-band σ_o variability for bare soil and heavy vegetation, using the [62] classification. The σ_o variability in vegetation is even less in specific regions, notably tropical rain forests.

RapidScat is now providing a precise characterization of the diurnal variation of radar backscatter over land. By nature of its non-synchronous orbit, RapidScat is the first scatterometer capable of observing σ_o over the full 24-hour cycle [63]. In addition, RapidScat has enabled improved rain forest cross- calibration between scatterometers operating at different local- times-of-day, e.g., [64].

To illustrate, the top panel of Fig. 8 shows the σ_o time series from 1998 to late 2015. In this figure, each point represents the Ku-band σ_o nearest to a location in the Amazon (the PR resolution is ≈4 km, so a 12 km x 12 km region is averaged to approximate the scatterometer footprint-level σ_o resolution), from the start of PR and into the GPM era (with the limited swath, the observations occurring once every 3-4 days). The mean is near -6 dB, with about ±1 dB variability, across all 17 years. The second panel shows the corresponding inner and outer-beam observations from QuikSCAT, OSCAT-1, and RapidScat, during each sensor's respective operating period. For each, the mean value is about 3 dB smaller, and the natural variability is somewhat larger than noted for PR/DPR. This suggests that despite these observational differences, the long record of PR/DPR observations over dense vegetation are useful for identifying unexpected changes to instrument operating characteristics. For example, beginning early in 2010 the OSCAT-1 σ_o dropped by about 0.5 to 1 dB, whereas the same fluctuations are not noted in the PR σ_o, suggesting that the change may be OSCAT-1-related. Indeed, this change in OSCAT-1 σ_o was related to a known 0.5 dB power drop in OceansSat-2 in August 2010 [65]. The bottom two panels of Fig. 8 show these same plots, but over a location in the Congo (0.47°N 21.57°E). Similar ranges in σ_o variability are observed, but the mean of each time series is shifted slightly (PR is slightly lower than was noted in the Amazon, whereas the scatterometer σ_o is slightly higher), owing to the different vegetation characteristics. This suggests the utility of the long- term, continuing record of Ku-band σ_o in the 12°-17° incidence angle range for calibrating the OSCAT-2 σ_o records over land, with due consideration for the diurnal cycle.

7. Specialized Model Assimilation of Satellite Winds

The objective of specialized model assimilations is to provide vector winds on a regularly spaced temporal/spatial grid while preserving the satellite wind information. These specialized assimilations mitigate the long-standing sampling limitations of constructing a composite ocean wind dataset from multiple satellites. These sampling issues include the fact that most of the satellite systems view the Earth at different local times, most are sensitive to precipitation, and many have no directional information. In contrast, much of the satellite wind information is filtered by large general-purpose numerical weather forecast models like ECMWF and NCEP, which generally lack deterministic mesoscale structure. Specialized assimilations fill the gap between single satellite products and the numerical weather forecast models. These Earth gridded vector winds greatly facilitate many science and operational applications.

Since the assimilation models resample or interpolate the satellite wind observations to regular (typically 6-hour) time intervals, this would be the ideal place to bring diurnal information into the processing stream. However, this will require a better understanding of the diurnal variations of winds over the world's oceans. In this regard, RapidScat is indispensable. RapidScat is the only scatterometer that views the ocean at all times of the day. The radiometers TMI and GMI provide diurnal wind speed information, which is certainly helpful, but much of the diurnal signal is characterized in terms of the U and V components of the wind field.

A. Advantages of Specialized Assimilations for OVW

The advantages of specialized assimilations for OVW include the following:

1. Specialized assimilations can take advantage of the full volume of microwave active and passive ocean winds, whereas only a small fraction is typically used in NWP assimilation systems.

2. Specialized assimilations can provide analysis on the smallest possible space and time scales. For examples, CCMP (described below) provides analyses every 6 hour with 25-km grid spacing over the world oceans. While CCMP resolves smaller scales than typical NWP products, it still has virtually no variability at scales smaller than O(200 Km) [66]. Since improved coverage would allow finer scale analyses, the Centre for Earth Observation satellites coordinates an Ocean Surface Vector Winds Virtual Constellation (OSVW VC) with the goal of improving spatial-temporal coverage.

3. Specialized assimilations can represent processes and detect new circulations and features not present in NWP fields. For example, ERA* described below adds additional information needed to depict essential dynamical processes including:

   a. Ocean eddy scale dynamics

   b. Air-sea interaction near moist convection

   c. Wind direction correction in stable atmospheric flow [67]

4. As a by-product, specialized assimilations can be used to assign directions to wind speed only data.

5. Specialized assimilations can be designed to provide consistent sets of wind stress and other fluxes.

B. Limitations of Specialized Assimilations for OVW

The main limitation on our knowledge of the OVW at scales of O(500 km) and greater is inhomogeneous sampling. There are regions and times where there are no satellite observations. There are also rain dropouts in the data swath. In many blended products, in case of no observations, a background field is used to fill in the data. For rain dropouts, moist convection is generally poorly represented in global NWP ([49]). In ERA* (described below) homogeneous sampling is achieved by computing local mean and variable adaptations to ERA over a few days. It must be recognized that satellite winds are relative to ocean currents rather than relative to a fixed Earth surface, as is the case for conventional observations and NWP backgrounds.

As the scale decreases below the O(500 Km) limit, the smoothing of natural variability becomes increasingly important. The lack of energy at small scales in the specialized assimilation could be corrected with statistical approaches [68], but for each time step the wind patterns on these small scales would not match the observed winds.

Another limitation of the use of specialized assimilations is the difficulty of maintaining the subtle decadal wind trends that are contained in the satellite observations. These trends can be small (0.1 m/s/decade) and can be distorted by the background field and by resampling. As one remedy, the satellite record can be used to monitor and correct for these types of systematic errors.

C. Technical Approach

In general, data assimilation methods seek the minimum of an objective function that measures the misfits of the analysis to observations, background, and constraints. This can also be true for specialized assimilations of OVW, including most examples listed below. Methods

differ in the details of the definition of the observation, background, and constraint functions, in what data are used, in the QC procedures that are applied, and in the solution method. Input data types may be radiances, backscatter measurements, retrieved wind speeds and/or retrieved wind directions. Retrieved quantities include some information from prior information used in the retrieval. This is accounted for in the analysis method, usually by tuning the weight given to these data. For OVW the QC usually eliminates observations affected by enhanced wind variability, precipitation and land and ice contamination. Typically, the solution method to find the minimizing analysis is based on the conjugate gradient approach. Using these techniques, several institutions have produced gridded wind products, which include the cross-calibrated multiplatform (CCMP, [66], the ERA* (a specialized version of ECMWF Reanalysis, [15]), and the OAFlux product [69] [70].

D. CCMP

The cross-calibrated multiplatform (CCMP) OVW dataset is one example of a long-term, high spatial/temporal resolution specialized assimilation [66]. CCMP is based on a proven, efficient variational analysis method (VAM) that is particularly well suited to the blending of different sources of ocean surface wind information in order to determine accurate high-resolution (O(200 Km) on a 25-km grid vector wind fields [66]. Note that the VAM analysis of satellite surface wind data adds small-scale variability to the ECMWF background ([66], Fig. SB1). Since much of the data used in CCMP processing are wind speeds from microwave radiometers, the VAM analyzed vector wind fields are used to assign directions to satellite wind speed observations. For the CCMP the input satellite data are the RSS cross-calibrated wind speeds derived from SSMI/SSMIS, TMI/GMI, AMSRE/AMSR2, and WindSat

and wind vectors are from QuikSCAT. The VAM combines all these satellite winds with conventional ship and buoy data and ECMWF reanalyses or operational analyses.

The CCMP OVWs (v1.1) for the period 1987 to 2011 are a community resource available through JPL's Physical Oceanography data archive. There are over 100 known references to work using CCMP OVWs in the refereed literature. CCMP v2.0 was recently released by RSS in January 2016 [71]. This re-processing and update of CCMP uses the most current and complete RSS cross-calibrated wind datasets—including ASCAT, uses the ECMWF Interim reanalysis as a consistent and higher resolution background, and extends the dataset to the present.

E. ERA*

The ECMWF Reanalysis (ERA) [72] is a convenient and consistent dynamical record of the atmosphere over the recent decades. ERA provides gridded fields every 3 hours (forecasts) or 6 hours (analyses). However, high-quality mesoscale wind observations, such as those from scatterometers and radiometers are rather poorly exploited. Spatial resolution is limited to a few 100 km over the open ocean due to its 80-km grid and dynamical closure (e.g., [73]). Therefore, essential dynamical characteristics of the air-sea interaction may be added by using satellite winds.

In ERA* these characteristics are added based on the evaluation of the systematic and varying difference of the satellite winds with respect to ERA [15]. To this end, differences between satellite observations and ERA are computed and locally their mean and standard deviation are stored. At any given location, the systematic effects and variances appear rather similar from day to day and depict the above model deficiencies in moist convection, PBL

closure and ocean currents. These statistics generally evolve slowly in time. The variance is mainly caused by moist convection, which dominates in the tropical moist convection regions, where its associated sea surface wind variability dominates the air-sea interaction [51]. The first year of ERA* will include ASCAT, and QuikSCAT will then follow at a different local ascending node time to test the effects of the diurnal cycle.

To produce ERA*, the evolving mean differences are applied as corrections to all ERA-interim stress-equivalent wind or derivative fields and thus constitute an improved representation of the abovementioned phenomena in ERA. Further perturbations to ERA are probably meaningful to represent the variance of the difference, constituting wind variability in convection areas. It is, in particular, this wind variability that is generally ignored, i.e., removed as noise, in other blended wind and stress products. ERA* is being verified against buoy winds and tested in ocean modeling [15]. Note that ERA* uses archived reanalysis background of stress-equivalent winds [74] and is provided 3-hourly.

To follow the data assimilation paradigm of Best Linear Unbiased Estimation, local observation wind biases should be removed before data assimilation. The method of ERA* may thus be applied to improve scatterometer data assimilation by a priori removing biases with the forecasting model. As dynamical wind biases settle within a few hours to the model- forced balance, these biases cannot be corrected effectively in data assimilation. Moreover, [67] demonstrate that it can be very complex to correct the forecasting model to the observed climatology. Therefore, for an effective dynamical initialization of forecasting models in data assimilation, it appears better to a priori remove local biases, e.g., using ERA* corrections [75].

F. Approaches under Development and Suggestions for Improvement

There is a middle ground between producing a regularly gridded field through purely statistical data assimilation and through an NWP reanalysis. The statistical methods can assimilate NWP products and it can include a constraint on the nearness of fit to reanalyses (e.g., CCMP); however, this approach makes the resulting product consistent with the comprehensive physical relationships imposed in the NWP assimilation. ERA* provides a middle ground, as it bridges the systematic effects imposed by data assimilation, by applying local corrections for bias and variability based on a statistical comparison and is not regulated by NWP constraints or other hard physical constraints.

Another such middle ground is a statistical approach that includes several of these physical constraints as hard constraints, or highly weighted soft constraints [76] [77]. Such an approach is being developed at FSU. One difficulty is that the link between the surface winds, Ekman winds, and geostrophic winds should apply globally. Previously, however, such constraints have not been applicable in both the tropics and the mid-latitudes (e.g., the University of Washington Planetary Boundary-Layer Model [78] [79]). A new constraint, based on the framework of [80] was extended to include all these layers. It has been modified to allow non-uniform zonal wind stress and non-zero temperature fronts, and has been shown to work in the tropics (as per [81]) and mid-latitudes (albeit currently as a rather time consuming calculation). Nevertheless, this constraint produces a smoother field that continues to include realistic features and much finer resolution than the statistical assimilation. Preliminary results have shown that this type of approach can roughly reproduce the observed dependence of spatial variability in wind as a function of the SST gradient. Such relationships are not found in NWP, except in a greatly weakened form. This dependency was not arbitrarily added, but rather is due to the

dynamics imposed by the hard constraint. Like NWP, this approach can also utilize wind speeds, surface pressures and temperatures to improve the wind fields. This middle approach is a promising alternative to more traditional approaches to producing regularly gridded fields.

Potential enhancements of specialized assimilations for OVW include the following:

- Use of archived reanalysis backgrounds. Note that modern NWP DA systems assimilate some of the in situ and satellite ocean winds that might be used in a specialized assimilation. ERA* uses archived reanalysis backgrounds (3, 6, 9 h forecasts) to avoid the potential double use of some of the observations and to provide 3 h temporal resolution.

- Use of additional data sources. Data from OSCAT-1 and OSCAT-2, RapidScat, CYGNSS, and other future sensors might be included in future specialized assimilations.

- Provide enhanced uncertainty estimates. Specialized assimilations should provide validated uncertainty estimates for each analysis quantity.

- Assimilation of non-wind variables. Since ocean surface winds, temperature and surface pressure and their gradients are co-varying, adding sea surface temperature and surface pressure information should improve the wind analysis.

8. Conclusions

A. Satellite sensors have been systematically measuring near-surface ocean winds for nearly 40 years, establishing an important legacy in studying and monitoring weather and climate variability. These wind measurements come from 13 active microwave scatterometers, which provide both speed and direction and 21 passive microwave radiometers, which only provide

wind speed (except for WindSat). These 34 sensors taken together and properly intercalibrated provide a highly accurate depiction of oceanic winds over several decades.

B. A number of institutions are constructing climate data records (CDR) of these ocean winds (OW). These OW-CDRs need to be maintained and periodically updated, with particular importance placed on the older datasets at the beginning of the record, which have received less attention than the more recent observations.

C. Looking to the future, ESA, ISRO, and CNSA have made commitments to continue wind scatterometry, but the same cannot be said for the continuation of microwave radiometers. The possible end of the 40-year wind speed record from spaceborne radiometers is of considerable concern. Currently there are no commitments for follow-on sensors to WindSat, GMI, or AMSR-2. The only scheduled radiometer, other than the CNSA MWRI, is the second-generation MetOp microwave imager (MWI), which will have limited wind-sensing capabilities and will not launch before 2022. Both MWRI and MWI have limited wind-sensing capabilities. The recent failures of the SSM/I on the F17 and the F19 DMSP spacecraft exacerbate this situation.

D. The need for absolute wind calibration via ocean buoys will continue into the future. Satellite wind sensors are not perfectly stable, and now that the time series of the OW-CDR is 3 decades, one must be concerned about small drifts (≈0.1 m/s) over 30 years. Buoys are indispensable in validating these decadal records of satellite winds. In this regard, requirements for buoy arrays (number and locations) to be used for satellite calibration need to be quantified and communicated to the TPOS 2020 Project.

E. Now that there are multiple versions of the OW-CDR at different institutions, the opportunity arises to compare these datasets with the objective of evaluating the uncertainties

associated with the construction of an OW-CDR. An OW Intercomparison Project is being formed as part of the IOVWST Climate Working Group to initiate these studies.

F. An example of extending the OW-CDR into the future is given for the inclusion of OSCAT-2 on ScatSat into the CDR. The various planned synergistic methods for intercalibrating the OSCAT-2 σ_o measurements are discussed, including (1) direct Ku-band σ_o intercalibration to QuikSCAT, (2) multi-sensor wind speed intercalibration, and (3) calibration to stable rainforest targets.

G. RapidScat is the only vector wind sensor that views the ocean throughout the complete 24-hour diurnal cycle. This unique capability has great potential for (1) cross-calibrating sun-synchronous sensors and (2) characterizing the diurnal variability of vector winds over the world's oceans. While there are other methods for cross-calibrating sun-synchronous sensors, there is no substitute for the diurnal vector wind information coming from RapidScat.

H. Specialized model assimilations can mitigate the long- standing problem of constructing a composite OVW dataset from multiple satellites viewing the Earth at different local times. The challenge is to remap the winds on a regularly spaced temporal/spatial grid while preserving the satellite wind information. The CCMP and ERA* methods produce widely used datasets, but additional research should be focused on more fully meeting this challenge.

References

[1] W. L. Jones, P. G. Black, D. M. Boggs, E. M. Bracalenta, R. A. Brown, G. Dome, J. A. Ernst, I. M. Halberstam, J. E. Overland, S. Peteherych, W. J. Person, F. J. Wentz, P. M. Woiceshyn and M. G. Wurtele, "Seasat Scatterometer: Results of tte Gulf of Alaska Workshop," *Science,* vol. 204, pp. 1413-1415, 1979.

[2] R. G. Lipes, R. L. Bernstein, V. J. Cardone, A. L. Riley, D. B. Ross, C. T. Swith and F. J. Wentz, "Seascat Scanning Multichannel Microwave Radiometer: Results of the Gulf of Alaska Workshop," *Science,* vol. 204, pp. 1415-1417, 1979.

[3] J. Jackson, Classical Electrodynamics, 2nd Edn., New York, John Wiley, 1975.

[4] T. Meissner and F. J. Wentz, "Polarization Rotation and the Third Stokes Parameter: The Effects of spacecraft attitude and Faraday rotation," *IEEE Transactions on Geoscience and Remote Sensing,* vol. 44, pp. 506-515, 2006.

[5] I. R. Young, S. Zieger and A. V. Babanin, "Global trends in wind speed and wave height," *Science,* vol. 332, no. 6026, pp. 451-455, 2011.

[6] F. J. Wentz, L. Ricciardulli, K. A. Hilburn and C. A. Mears, "How much more rain will global warming bring? *Science,* vol. 317, pp. 233-235, 2007.

[7] F. J. Wentz and L. Ricciardulli, "Comment on "Global trends in wind speed and wave height," *Science,* vol. 334, no. 6058, p. 905, 2011.

[8] I. Young, A. V. Babanin and S. Zieger, "Response to Comment on Global trends in wind speed and wave height," *Science,* vol. 334, no. 6058, p. 905, 2011.

[9] World Meteorological Organization, "Systematic Observation Requirements for Satellite-based Products for Climate Supplemental details to the satellite-based component of the Implementation Plan for the Global Observing System for Climate in Support of the UNFCCC (2011 Update)," World Meteorological Organization - GCOS 154, Geneva 2, Switzerland, 2011.

[10] F. J. Wentz, "SSM/I Version-7 Calibration Report. RSS Technical Report 011012," Remote Sensing Systems, Santa Rosa, 2013.

[11]   F. J. Wentz, "A 17-year climate record of environmental parameters derived from the Tropical Rainfall Measuring Mission (TRMM) Microwave Imager," *Journal of Climate,* vol. 28, pp. 6882-6902, 2015.

[12]   F. J. Wentz and D. Draper, "On-orbit absolute calibration of the Global Precipitation Mission Microwave Imager," *Journal of Atmospheric and Oceanic Technology,* vol. 33, pp. 1393-1412, 2016.

[13]   F. J. Wentz and L. Ricciardulli, "Improvements to the Vector Wind Climate Record Using RapidScat as a Common Reference and Aquarius/SMAP for High Winds in Rain, RSS Technical Report 111313," Remote Sensing Systems, Santa Rosa, 2013.

[14]   L. Ricciardulli and F. J. Wentz, "A scatterometer geophysical model function for climate-quality winds: QuikSCAT Ku-2011," *Journal of Atmospheric and Oceanic Technology,* vol. 32, pp. 1829-1846, 2015.

[15]   A. Stoffelen, A. Verhoef, J. de Kloe and Coauthors, "Scatterometer Stress-Equivalent Winds for Ocean and Climate Applications," in *EUMETSAT User Conference*, Toulouse, France, 2015.

[16]   A. Verhoef and CoAuthors, "Long term climatological data records from scatterometer winds," *Journal of Selected Topics in Applied Earth Observations and Remote Sensing (J-STARS), this issue,* 2016.

[17]   Remote Sensing Systems, "ASCAT Version 2.1 Data Release/QSCAT" Remote Sensing Systems.

[18]   Royal Netherlands Meteorological Institute, "2016: OSI SAF Reprocessed SeaWinds L2 winds," Ocean and Sea Ice SAF Wind Processing Centre.

[19]   M. Belmonte Rivas, A. Stoffelen, A. Verspeek, A. Verhoef and C. Anderson, "Cone metrics: a new tool for the inter-calibration of scatterometer records," *Journal of Selected Topics in Applied Earth Observations and Remote Sensing (J-STARS), this issue,* 2016.

[20]   S. T. Gille, G. L. Smith and S. M. Lee, "Measuring the Sea Breeze from QuikSCAT scatterometry," *Geophysical Research Letters,* vol. 30, no. 3, p. 1114, 2003.

[21] S. T. Gille, "Statistical Characterization of Zonal and Meridional Ocean Wind Stress," *Journal of Atmospheric and Oceanic Technology,* vol. 22, pp. 1353-1372, 2005.

[22] R. Ueyama and C. Deser, "A Climatology of Diurnal and Semidiurnal Surface Wind Variations Over the Tropical Pacific Ocean Based on the Tropical Atmosphere Ocean Moored Buoy Array," *Journal of Climate,* vol. 21, pp. 593-607, 2008.

[23] R. M. Wood, M. Köhler, R. Bennartz and C. O'Dell, "The diurnal cycle of surface divergence over the global oceans," *Quarterly Journal of the Royal Meteorological Society,* vol. 135, pp. 1484-1493, 2009.

[24] K. Li, M. A. Bourassa and S. R. Smith, "Adjustment of visually observed ship winds (Beaufort winds) in ICOADS," in *poster presented at 2015 International Ocean Vector Winds Science Team Meeting*, Portland, OR, May 19-21, 2015.

[25] C. W. Fairall, G. S. Young, E. F. Bradley, D. P. Rogers and J. B. Edson, "Bulk parameterization of air-sea fluxes for Tropical Ocean-Global Atmosphere Coupled-Ocean Atmosphere Response Experiment," *Journal of Geophysical Research,* vol. 101, pp. 3747-3764, 1996.

[26] C. W. Fairall, E. F. Bradley, J. E. Hare, A. A. Grachev and J. B. Edson, "Bulk parameterization of air–sea fluxes: Updates and verification for the COARE algorithm," *Journal of Climate,* vol. 16, pp. 571-591, 2003.

[27] A. Plagge, D. Vandemark and B. Chapron, "Examining the impact of surface currents on satel-lite scatterometer and altimeter ocean winds," *Journal of Atmospheric and Oceanic Technology,* vol. 29, pp. 1776-1793, 2012.

[28] L. Zeng and R. A. Brown, "Scatterometer observations at high wind speeds," *Journal of Applied Meteorology,* vol. 37, pp. 1412-1420, 1998.

[29] W. G. Large, J. Morzel and G. B. Crawford, "Accounting for surface wave distortion of the marine wind profile in low-level ocean storms wind measurements," *Journal of Physical Oceanography,* vol. 25, pp. 2959-2971, 1995.

[30] P. K. Taylor and M. J. Yelland, "On the Effect of Ocean Waves on the Kinetic Energy Balance and Consequences for the Inertial Dissipation Technique," *Journal of Physical Oceanography,* vol. 31, pp. 2532-2536, 2001.

[31] S. Howden, D. Gilhousen, N. Guinasso, J. Walpert, M. Sturgeon and L. Bender, "Hurricane Katrina winds measured by a buoy-mounted sonic anemometer," *Journal of Atmospheric and Oceanic Technology,* vol. 25, pp. 607-616, 2008.

[32] J. B. Edson and CoAuthors, "On the exchange of momentum over the open ocean," *Journal of Physical Oceanography,* vol. 43, pp. 15-89-1610, 2013.

[33] J. Verspeek, J. A. Stoffelen, M. Portabella, H. Bonekamp, C. Anderson and J. F. Saldana, "Validation and calibration of ASCAT using CMOD5.n," *IEEE Transactions on Geoscience and Remote Sensing,* vol. 48, pp. 386-395, 2010.

[34] W. Lin, M. Portabella and A. Stoffelen, "On the characteristics of ASCAT wind direction ambiguities," *Atmospheric Measurement Techniques Discussions,* vol. 5, pp. 8839-8857, 2012.

[35] M. Portabella, A. Stoffelen, W. Lin, A. Turiel, A. Verhouf, J. Verspeek and J. Ballabrera-Poy, "Rain effects on ASCAT-retrieved winds: Toward an improved quality control," *IEEE Transactions on Geoscience and Remote Sensing,* vol. 50, pp. 2495-2506, 2012.

[36] L. W. O'Neill, T. Haack and T. Durland, "Estimation of time-averaged surface divergence and vorticity from satellite ocean vector winds," *Journal of Climate,* vol. 28, pp. 7596-7620, 2015.

[37] A. Stoffelen, J. Vogelzang and W. Lin, "On buoys, scatterometers and reanalyses for globally representative winds, KNMI Document NWPSAF-KN-TR-024," The EUMETSAT Network of Satellite Application Facilities, 2015.

[38] A. Stoffelen, "Toward the true near-surface wind speed: Error modeling and calibration using triple collocation," *Journal of Geophysical Research,* vol. 103, pp. 7755- 7766, 1998.

[39] K. A. McColl, J. Vogelzang, A. G. Konings, D. Entekhabi, M. Piles and A. Stoffelen, "Extended triple collocation: Estimating errors and correlation coefficients with respect to an unknown target," *Geophysical Research Letters,* vol. 41, pp. 6229-6236, 2014.

[40] J. May and M. A. Bourassa, "Quantifying variance due to temporal and spatial difference between ship and satellite winds," *Journal of Geophysical Research,* vol. 116, 2011.

[41] J. Verspeek and A. Stoffelen, "ASCAT-A anomalies in September and October 2014," EUMETSAT Ocean and Sea Ice SAF report: SAF/OSI/CDOP2/KNMI/TEC/RP/236, 2015.

[42] L. Ricciardulli, "ASCAT on Metop-A Data product update notes: V2.1 data release," Technical Report 040416, Remote Sensing Systems, Santa Rosa, CA, Usa, 2016.

[43] T. R. Karl, S. J. Hassol, C. D. Miller and W. L. Murray, "Temperature trends in the lower atmosphere: Steps for understanding and reconciling differences," U.S. Climate Change Science Program and the Subcommittee on Global Change Research Final Report, Washington, D.C.

[44] P. W. Thorne, T. C. Lanzante, T. C. Peterson, D. J. Seidel and K. P. Shine, "Tropospheric temperature trends: history of an ongoing controversy," *Wiley Interdisciplinary Reviews: Climate Change,* vol. 2, no. 1, pp. 66-88, 2011.

[45] D. J. Seidel, J. Li, C. Mears, I. Moradi, J. Nash, W. J. Randel, R. Saunders, D. W. J. Thompson and C. -Z. Zou, "Stratospheric temperature changes during the satellite era," *Journal of Geophysical Research-Atmospheres,* vol. 121, no. 2, pp. 664-681, 2016.

[46] D. G. Draper and D. W. Long, "Simultaneous Wind and rain retrieval using SeaWinds data," *IEEE Transactions on Geoscience and Remote Sensing,* vol. 42, pp. 411-1423, 2004.

[47] C. Nie and D. G. Long, "A C-band Scatterometer Simultaneous Wind/Rain Retrieval Method," *IEEEE Transactions on Geoscience and Remote Sensing,* vol. 46, pp. 3618-3632, 2009.

[48] A. G. Fore, B. W. Stiles, A. H. Chau, B. A. Williams, R. S. Dunbar and E. Rodriguez, "Point-wise wind retrieval and ambiguity removal improvements for the QuikSCAT climatological data set," *IEEE Transactions on Geoscience and Remote Sensing,* vol. 52, no. 1, pp. 51-59, 2014.

[49] L. Ricciardulli and F. Wentz, "Progress and future plans on an ocean vector wind climate record," in *presented at the International Ocean Vector Wind Science Team meeting*, Brest, France, 2014.

[50] W. Lin, M. Portabella, A. Stoffelen, A. Turiel and A. Verhoef, "Rain identification in ASCAT winds using singularity analysis," *IEEE Geoscience and Remote Sensing Letters,* vol. 11, pp. 1519-1523, 2014.

[51] W. Lin, A. Portabella, A. Stoffelen, A. Verhoef and A. Turiel, "ASCAT wind quality control near rain," *IEEE Transactions on Geoscience and Remote Sensing,* vol. 53, pp. 4165-4177, 2015.

[52] R. J. Joyce, J. E. Janowiak, P. A. Arkin and P. Xie, "CMORPH: A method that produces global precipitation estimates from passive microwave and infrared data at high spatial and temporal resolution," *Journal of Hydrometeorology,* vol. 5, pp. 487-503, 2004.

[53] F. J. Wentz and CoAuthors, "Evaluating and Extending the Ocean Wind Climate Data Record," *Remote Sensing Systems,* vol. 10, no. 5, pp. 2165-2185, 2017.

[54] D. B. Chelton and M. H. Freilich, "Scatterometer-based assessment of 10-m wind analyses from the operational ECMWF and NCEP numerical weather prediction models," *Monthly Weather Review,* vol. 133, pp. 409- 429, 2005.

[55] Q. D. Redmind and D. G. Long, "A decade of QuikSCAT scatterometer sea ice extent data," *IEEE Transactions on Geoscience and Remote Sensing*, vol. 52, no. 7, pp. 4281-4290, 2014.

[56] D. B. Lindell and D. G. Long, "Multiyear arctic sea ice classification using OSCAT and QuikSCAT," *IEEE Transactions on Geoscience and Remote Sensing,* vol. 54, pp. 167-175, 2016.

[57] S. Nghiem, B. D. Wardlow, D. Allured, M. D. Svoboda, D. LeComte, M. Rosencrans, S. Chan and G. Neumann, "Microwave remote sensing of soil moisture: Science and applications," in *Microwave Remote Sensing of Drought: Innovative Monitoring Approaches*, Boca Raton, FL, CRC Press, 2012, pp. 197-226.

[58] F. J. Turk, R. Sikhakolli, P. Kirstetter and S. L. Durden, "Exploiting over-land OceanSat-2 scatterometer observations to capture short-period time-integrated precipitation," *Journal of Hydrometeorology,* vol. 16, pp. 2519-2535, 2015.

[59]   S. A. Bhowmick, R. Kumar and A. S. K. Kumar, "Cross calibration of the OceanSAT-2 scatterometer with QuikSCAT scatterometer using natural terrestrial targets," *IEEE Transactions on Geoscience and Remote Sensing,* vol. 52, pp. 3393-3398, 2014.

[60]   H. Stephen and D. G. Long, "Multi-spectral analysis of the Amazon basin using SeaWinds, ERS, Seasat scatterometers, TRMM-PR and SSM/I," in *2002 IEEE International Geoscience and Remote Sensing Symposium*, Toronto, Canada, 2002.

[61]   R. Meneghini and J. A. Jones, "Standard deviation of spatially averaged surface cross section data from the TRMM Precipitation Radar," *IEEE Geoscience and Remote Sensing Letters,* vol. 8, pp. 293-297, 2011.

[62]   S. L. Durden, S. Tanelli and R. Meneghini, "Using surface classification to improve surface reference technique performance over land," *Indian Journal of Radio & Space Physics,* vol. 41, pp. 403-410, 2012.

[63]   A. P. Paget, D. G. Long and N. M. Madsen, "RapidScat diurnal cycles over land," *IEEE Transactions on Geoscience and Remote Sensing,* vol. 54, no. 6, pp. 3336-3344, 2016.

[64]   N. M. Madsen and D. G. Long, "Calibration and validation of the RapidScat Scatterometer Using Tropical Rainforests," *IEEE Transactions on Geoscience and Remote Sensing,* vol. 54, no. 5, pp. 2846-2854, 2016.

[65]   S. Jaruwatanadilok, B. W. Stiles and A. G. Fore, "Cross- calibration between QuikSCAT and Oceansat-2," *IEEE Transactions on Geoscience and Remote Sensing,* vol. 52, pp. 6197-6204, 2013.

[66]   R. M. Atlas, R. N. Hoffman, J. Ardizzone, S. M. Leidner, J. C. Jusem, D. K. Smith and D. Gombo, "A cross-calibrated, multi-platform ocean surface wind velocity product for meteorological and oceanographic applications," *Bulletin of the American Meteorological Society,* vol. 92, pp. 157-174, 2011.

[67]   I. Sandu, A. Beliaars, P. Bechtold, T. Mauritsen and G. Balsamo, "Why is it so difficult to represent stably stratified conditions in numerical weather prediction (NWP) models?," *Journal of Advances in Modeling Earth Systems,* vol. 5, pp. 117-133, 2013.

[68]   T. M. Chin, R. F. Milliff and W. G. Large, "Basin-scale, high-wavenumber sea surface wind fields from a multiresolution analysis of scatterometer data," *Journal of Atmospheric and Oceanic Technology,* vol. 15, pp. 741-763, 1998.

[69]   L. Yu and X. Jin, "Insights on the OAFlux ocean surface vector wind analysis merged from scat-terometers and passive microwave radiometers (1987 onward)," *Journal of Geophysical Research: Oceans,* vol. 119, pp. 5244- 5269, 2014.

[70]   L. Yu and X. Jin, "Confidence and sensitivity study of the OAFlux multi- sensor synthesis of the global ocean surface vector wind from 1987 onward," *Journal of Geophysical Research: Oceans,* vol. 119, pp. 6842-6862, 2014.

[71]   F. J. Wentz, J. Scott, R. Hoffman, M. Leidner, R. Atlas and J. Ardizzone, "Remote Sensing Systems Cross- Calibrated Multi-Platform (CCMP) 6-hourly ocean vector wind analysis product on 0.25 deg grid, Version 2.0, [indicate date subset, if used]," Remote Sensing Systems, Santa Rosa, CA, 2015.

[72]   D. P. Dee and CoAuthors, "The ERA-Interim reanalysis: Configuration and performance of the data assimilation system," *Quarterly Journal of the Royal Meteorological Society,* vol. 137, pp. 533-597, 2011.

[73]   J. Vogelzang, A. Stoffelen, A. Verhoef and J. Figa- Saldaña, "On the quality of high-resolution scatterometer winds," *Journal of Geophysical Research,* vol. 116, 2011.

[74]   de Kloe and CoAuthors, "TBD," *Journal of Selected Topics in Applied Earth Observations and Remote Sensing (J-STARS), this issue,* 2016.

[75]   A. Stoffelen and CoAuthors, "C-band scatterometry: scientific challenges and opportunities from the new scatterometers in Metop-SG," *Journal of Selected Topics in Applied Earth Observations and Remote Sensing (J- STARS), this issue,* 2016.

[76]   B. J. Hicks, A. J. Medland and G. Mullinex, "Hicks, B. The representation and handling of constraints for the design, analysis and optimization of high speed machinery," *Artificial Intelligence for Engineering Design, Analysis and Manufacture (AIEDAM),* vol. 20, pp. 313-328, 2006.

[77]   J. Kendall, "Hard and soft constraints in linear programming," *Omega,* vol. 3, pp. 709-715, 1975.

[78] J. Patoux and R. A. Brown, "A gradient wind correction for surface pressure fields retrieved from scatterometer winds," *Journal of Applied Meteorology,* vol. 41, pp. 133-143, 2002.

[79] J. Patoux and R. A. Brown, "Global pressure fields from scatterometer winds," *Journal of Applied Meteorology,* vol. 42, pp. 813-826, 2002.

[80] H. Stommel, "Wind-drift near the equator," *Deep Sea Research,* vol. 6, pp. 298-302, 1953.

[81] F. Bonjean and G. S. Lagerloef, "Diagnostic model and analysis of the surface currents in the tropical Pacific Ocean," *Journal of Physical Oceanography,* vol. 32, pp. 2938-2954, 2002.
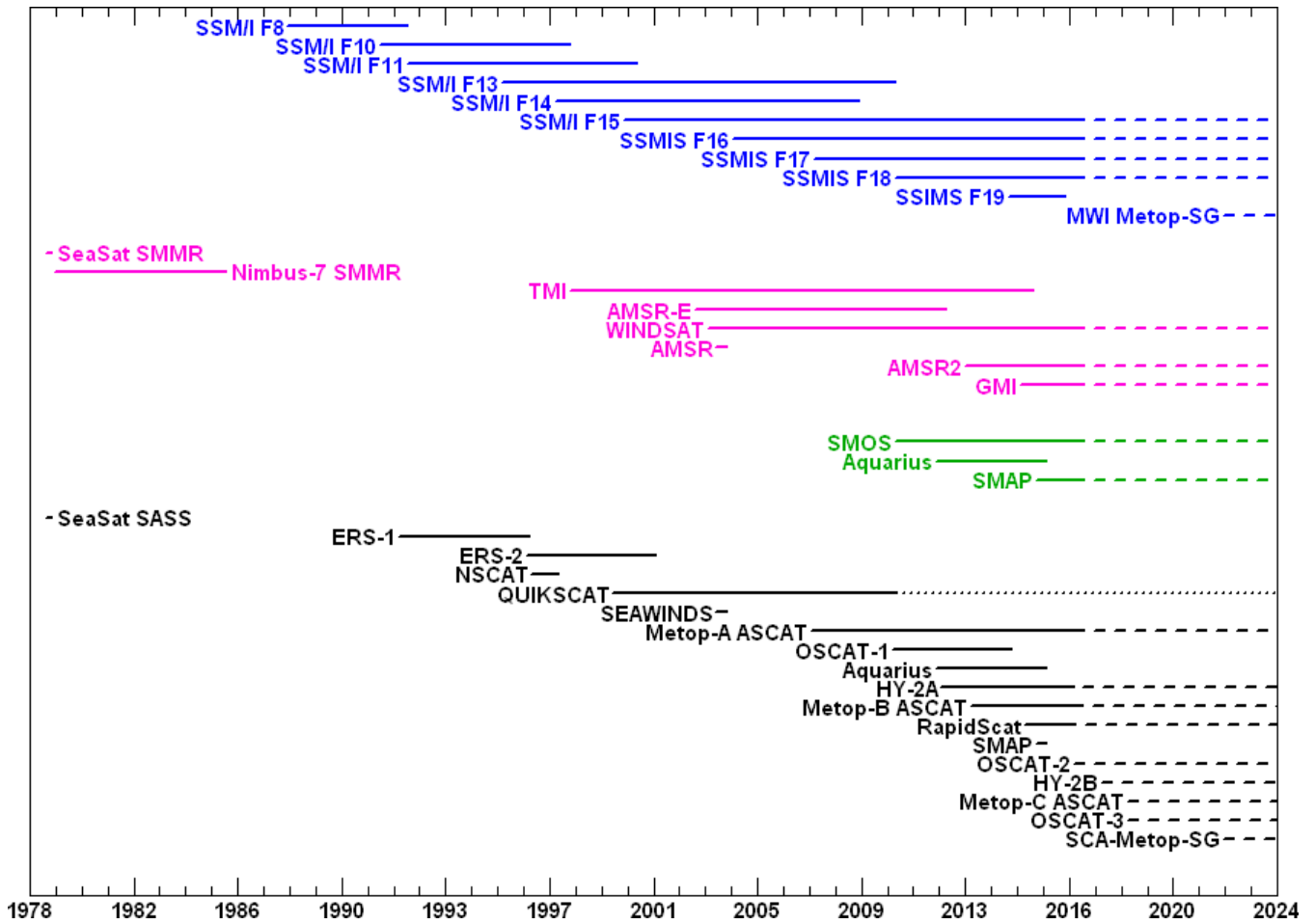
Figure 1. Four decades of satellite wind measurements and scheduled future missions. The black lines show the series of microwave scatterometers that provide ocean vector winds (OVW). After HY-2B, CNSA plans to fly scatterometers not shown. The dotted line extending the QuikSCAT from 2009 onward denotes the non-spinning phase of operation. The blue lines show the SSM/I and SSMIS instruments flown on the series of DMSP satellite platforms numbered F8 to F20. These sensors only provide ocean wind speed, not direction. The pink lines show the microwave radiometers with the lower frequency channels needed for measuring sea surface temperatures in addition to wind speed, water vapor, clouds and rain rates. The lower frequency channels also improve the wind speed accuracy. WindSat is the only microwave radiometer that also provides wind direction due to the inclusion of polarimetric channels. The green lines show the L- band radiometers SMOS, Aquarius and SMAP, which are very insensitive to rain and especially well-suited for measuring high winds in storms.
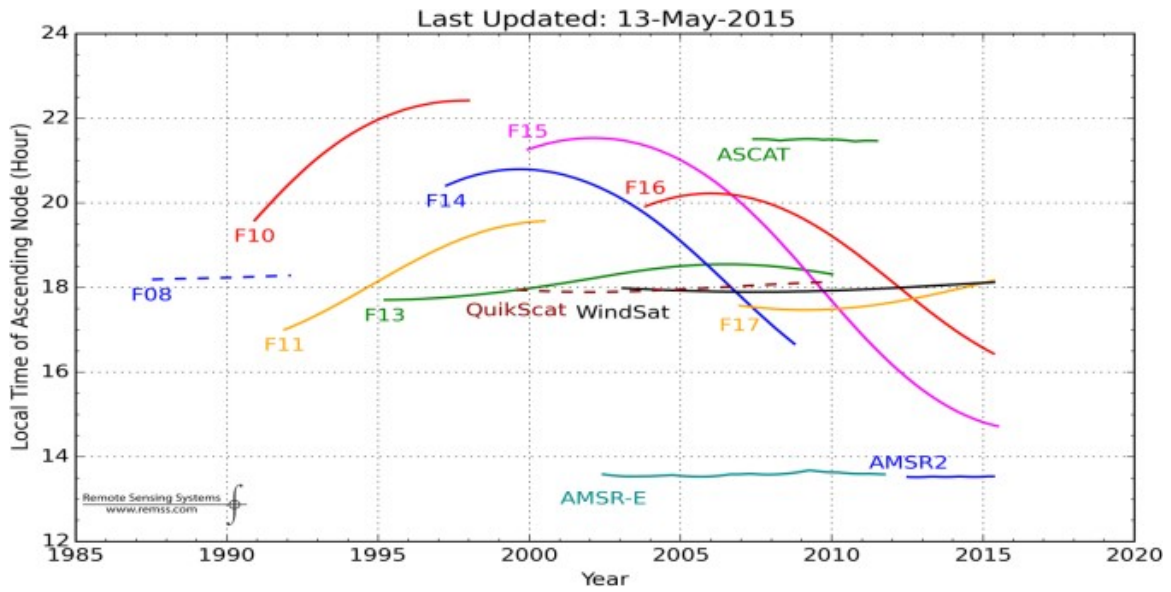
Figure 2. An example of the local time of the ascending node for some of the sun-synchronous scatterometer and radiometer wind observations, from 1988 until present (solid lines). QuikSCAT and F08 (dash lines) differ in that their descending node is plotted. Sensors with rapidly precessing orbits (TMI, GMI, and RapidScat) are not shown in the figure.
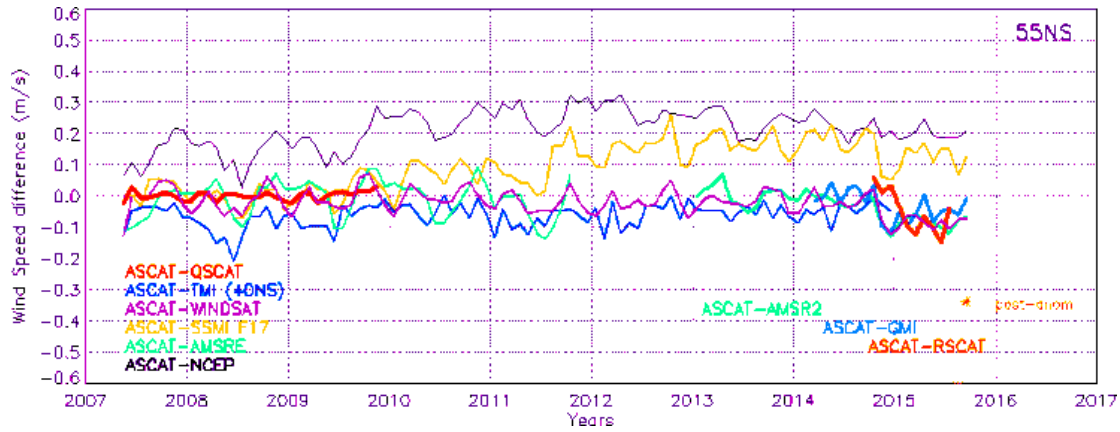
Figure 3. Global monthly time series of the rain-free wind speed differences between the ASCAT-A and the following sensors collocated to within four hours: QuikSCAT, TMI, WindSat, AMSRE, SSMI F17, AMSR2, GMI, and RapidScat. All of these satellite wind timeseries are RSS CDR products except for RapidScat (RSCAT), which is produced at JPL. NCEP GDAS model winds are also compared. The red star at the end of 2015 represents the ASCAT-RapidScat in the days after the hardware anomaly in August 2015. Note that the F17 SSM/I has a known wind speed drift which started in mid- 2011. The origin of this drift is currently under investigation. Also, NCEP timeseries is not stable due to the frequent changes in the datasets it assimilates. As discussed in section V.C , a calibration shift is apparent between ASCAT-A (version V1 displayed here) and the other datasets in September 2014. The data have now been reprocessed (version V2.1, [42]) taking into account a calibration adjustment provided by KNMI [41].
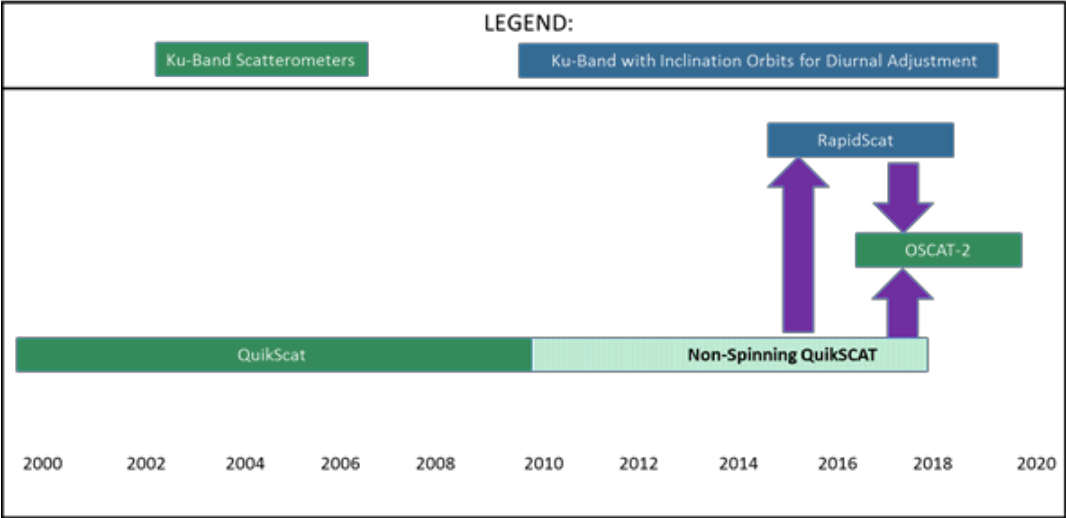
**Figure 4.** Existing and planned direct intercalibration of Ku-band σ_o measurements.
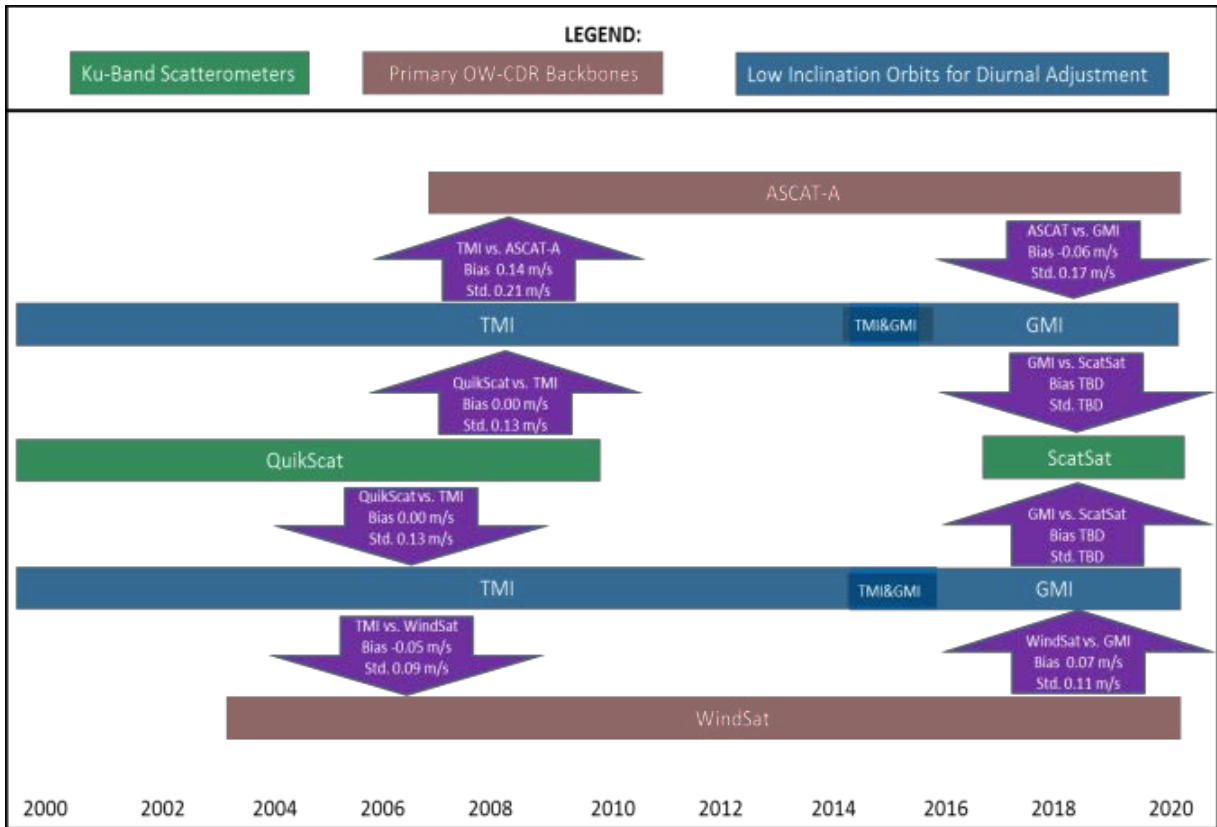
Figure 5. Multiple paths for wind speed intercalibration. The bias and standard deviation are found by averaging over the pixels in the 1° latitude/longitude annual map of the wind speed difference.
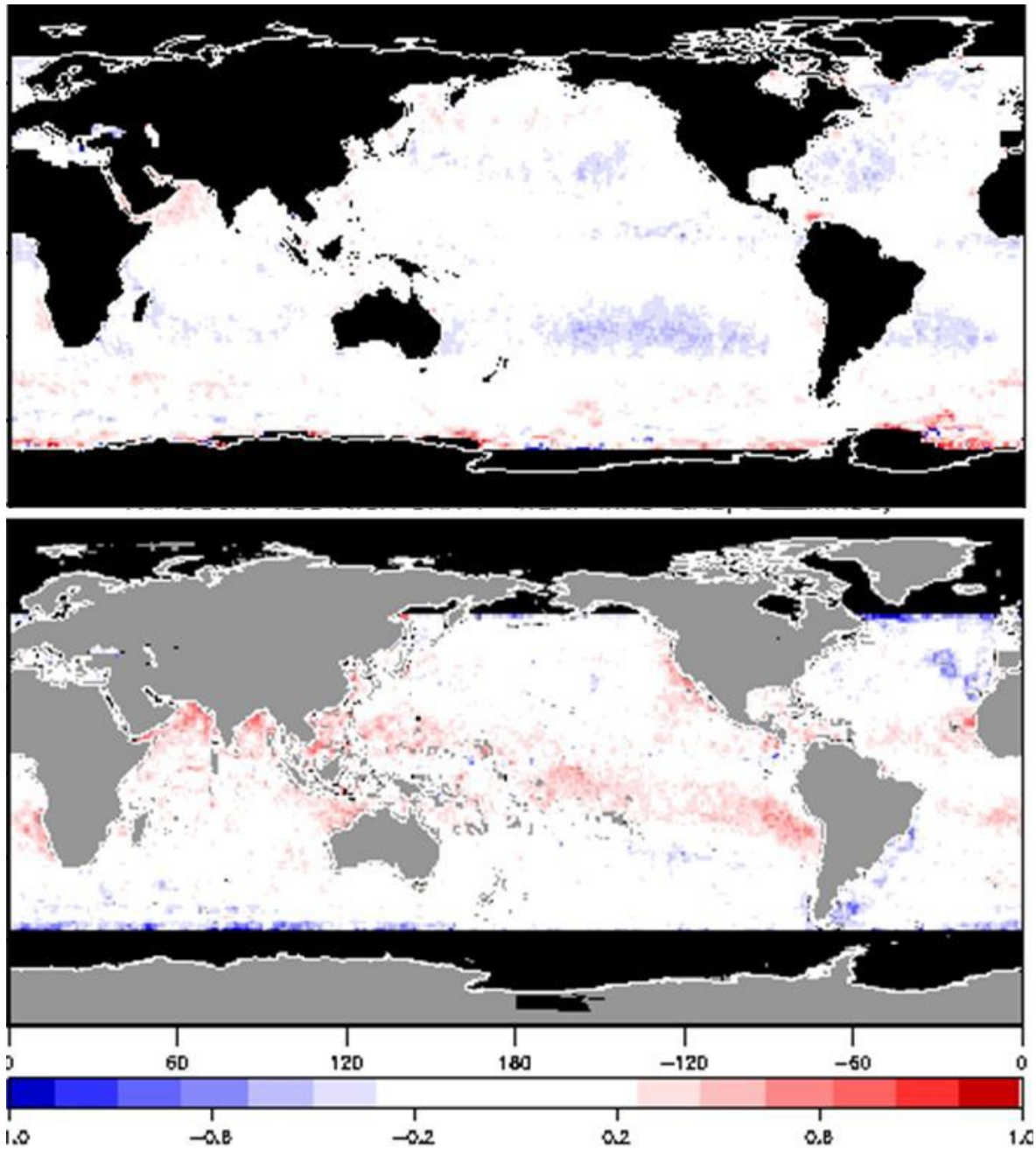
Figure 6. Wind speed differences of ASCAT-A minus GMI (top panel) and RapidScat minus WindSat (bottom panel). The ASCAT-A/GMI results are a 2-year average (2014-2015), and the time collocation is 2 hours. The RapidScat/WindSat results are averaged from October 2014 to August 2015 (i.e., up until the RapidScat gain anomaly), and the time collocation window is 1.5 hours. Color scale is in units of m/s.
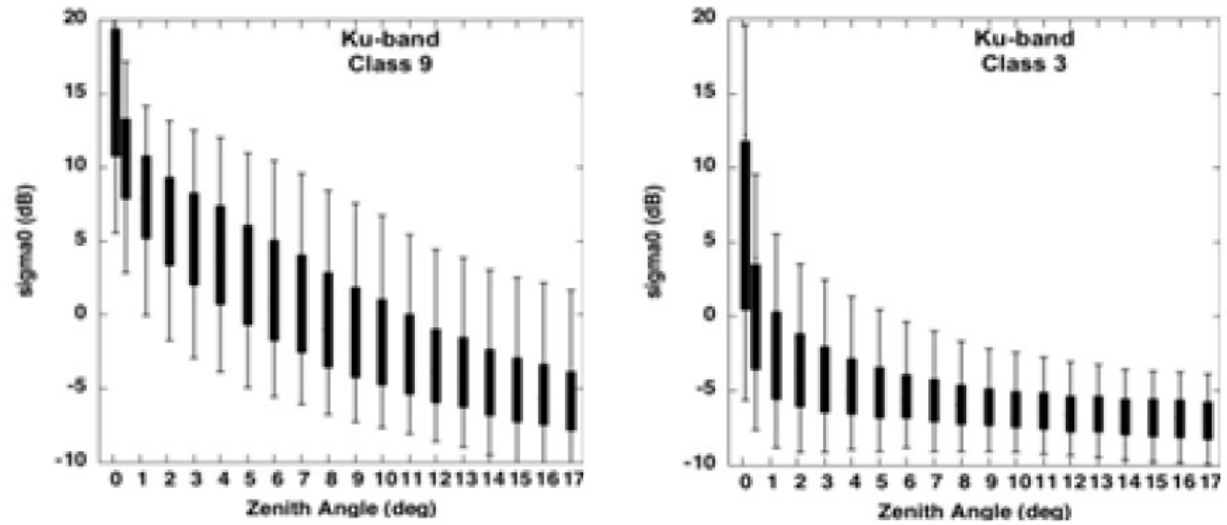
Figure 7. Box-and-whisker figures illustrating the variability (5, 25, 75 and 95 percent quartile) of the Ku-band DPR backscatter over bare soil (left) and dense vegetation (right) at incidence angles up to 17° from nadir, using the Durden classification [62].
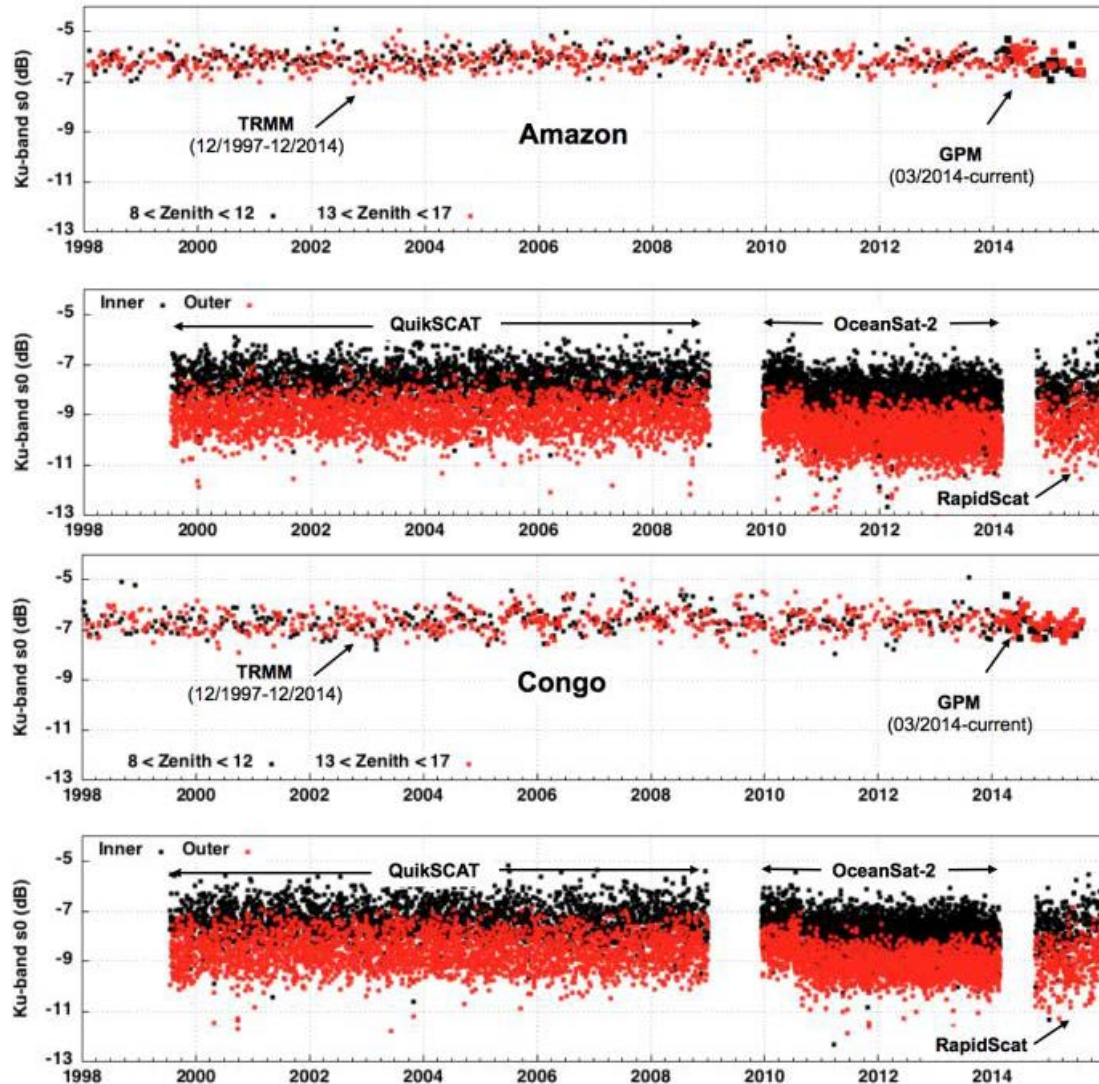
Figure 8. (Top) Time series from 1998 to late 2015 for TRMM Precipitation Radar and GPM Dual-Frequency Precipitation Radar surface backscatter cross section, and the individual periods of record for each of QuikSCAT, OSCAT- 1, and RapidScat, for a location in the Amazon (2.41S 63.15W). Black is for lower zenith angles and red for higher zenith angles as indicated in each panel. (Bottom) Same as top panels, but for a location in the Congo (0.47°N 21.57°E).

58

Table 1: Current and future global scatterometer vector wind datasets.

Instrument	Document Reference	Time Period	Production Institutions
SeaSat SASS	SASS	Jul – Oct 1978	JPL
ERS-1 AMI-SCAT	ERS-1	Jul 1991 – Apr 1996	ESA, KNMI
ERS-2 AMI-SCAT	ERS-2	Apr 1995 – Jun 2003	ESA, KNMI
ADEOS-1 NSCAT	NSCAT	Sep 1996 – Jun 1997	JPL, RSS
ADEOS-II SeaWinds	SeaWinds	Dec 2002 – Oct 2003	JPL, RSS
QuikSCAT SeaWinds	QuikSCAT	Jun 1999 – Nov 1999	JPL, RSS, KNMI
Metop-A ASCAT	ASCAT-A	Oct 2006 – present	KNMI, RSS
Metop-B ASCAT	ASCAT-B	Sep 2012 – present	KNMI
Metop-C ASCAT	ASCAT-C	2018 (planned)	KNMI
Aquarius Scatterometer	Aquarius	Jun 2011 – June 2015	JPL, RSS
ISS RapidScat*	RapidScat	Oct 2014 – Aug 2016	JPL, KNMI
OSCAT-1	Oceansat-2	Sep 2009 – Feb 2014	ISRO, KNMI, JPL
OSCAT-2	ScatSat	Sep 2016 – present	ISRO, KNMI, JPL
OSCAT-3	Oceansat-3	2018 (planned)	ISRO, KNMI, JPL
HY-2A Scat	HY-2A	Jun 2011 – present	NSOAS, CAST, KNMI
HY-2B Scat	HY-2B	2017 (planned)	NSOAS, CAST
SMAP Radar	SMAP	Feb – Jul 2015	JPL
Metop-SG SCA	SCA	2022 (planned)	ESA

*Non-sun-synchronous

Table 2: Current and future global radiometer wind speed datasets.

Instrument	Document Reference	Time Period	Production Institutions
SeaSat SMMR	SMMR-1	Jul – Oct 1978	RSS
Nimbus-7 SMMR	SMMR-2	Nov 1978 – Oct 1984	RSS
F08 SSM/I	F08	Jul 1987 – Dec 1991	RSS
F10 SSM/I	F10	Dec 1990 – Nov 1997	RSS
F11 SSM/I	F11	Dec 1991 – May 2000	RSS
F13 SSM/I	F13	May 1995 – Nov 2009	RSS
F14 SSM/I	F14	May 1997 – Aug 2008	RSS
F15 SSM/I	F15	Dec 1999 – present	RSS
F16 SSMIS	F16	Oct 2003 – present	RSS
F17 SSMIS	F17	Dec 2006 – present	RSS
F18 SSMIS	F18	Oct 2009 – present	RSS
F19 SSMIS	F19	Apr 2014 – Feb 2016	RSS
TRMM TMI*	TMI	Nov 1997 – Apr 2015	RSS
ADEOS-II AMSR	AMSR	Dec 2002 – Oct 2003	RSS, JAXA
AQUA AMSR-E	AMSRE	May 2002 – Oct 2011	RSS, JAXA
GCOM-W1 AMSR2	AMSR2	May 2012 – present	RSS, JAXA
Coriolis WindSat^	WindSat	Jan 2003 – present	RSS, NRL
GPM GMI*	GMI	Feb 2014 – present	RSS
Aquarius	Aquarius	Jun 2011 – Jun 2015	RSS, JPL
SMAP^	SMAP	Jan 2015 – present	RSS, JPL
SMOS MIRAS	SMOS	Nov 2009 – present	ESA
Metop-SG MWI	MWI	2022 (planned)	ESA

*Non-sun-synchronous

^Wind direction also

Table 3: Planned calibration procedures for extending the OVW-CDR to OSCAT-2. Note that RapidScat failed in August 2016. Although it cannot be directly used to calibrate OSCAT-2, the diurnal information provided by RapidScat will be indispensable.

Calibration Choice	Advantages	Limitations
QuikSCAT	- Measures σ_o at same incidence and polarization - Has proven long-term stability - σ_o calibration independent of geophysical model function - Calibration within 0.1 dB in 1 month	- One azimuth angle and narrow swath - Requires 3 months averaging for 0.05 dB calibration, 6 months to observe trends - Does not sample at the same time - Wind retrievals not possible without independent direction information
RapidScat	- Provides measurements simultaneous in time - Provides wide swath Ku-band winds - Rainforest calibration unaffected by low SNR state: can monitor Amazon drift - Provides a direct way of cross-calibrating sun-synchronous satellites - ISS availability through summer 2017	- Low SNR state has unknown long-term stability - Current stability estimates will require multiple months for calibration
ASCAT	- Proven stability and known wind performance - Local times similar to OSCAT-2 during ScatSat early phase - Ku and C-band intercalibrated through RapidScat-ASCAT comparisons	- Cannot provide direct Ku σ_o stability assessment over land and ice - Subject to GMF limitations and changes - Small regional differences exist between the C and Ku band winds
Radiometers	- Availability of long-term wind speed CDR among many different platforms - Diversity of local times - Consistency among sensors better than 0.1 m/s - Several sensors available for OSCAT-2 calibration (GMI, WindSat, AMSRS)	- Subject to GMF limitations and changes - Cannot be used to validate directions or derivatives
Land calibration	- Provides long-term continuity between instruments - Typical σ_o variability is small	- Provides a drift reference, but not absolute calibration - Could vary in the near term due to El Niño induced drought - 0.7 dB diurnal cycle
NWP model	- Consistent wind reference for multiple platforms - Trends can be assessed against buoy network	- Long term biases can be introduced as data being ingested or methodology changes - Cannot resolve with sufficient resolution to validate divergence or curl - NWP models have distorted representation of the diurnal signal

Table 4: Globally averaged wind speed difference of RapidScat versus four other satellite wind sensors. RapidScat winds are calibrated to agree with the average results obtained from the four comparison sensors.

Validation Instrument	Wind Speed Difference (m/s)
RapidScat-GMI	0.05
RapidScat-WindSat	-0.02
RapidScat-ASCAT-A	-0.03
RapidScat-AMSR2	-0.01